ACOUSTICALLY ACTIVATED RELEASE OF ESTRONE-TARGETED LIPOSOMES USED FOR BREAST CANCER TREATMENT

by

Najla Mohammad

A Thesis Presented to the Faculty of the
American University of Sharjah
College of Engineering
in partial Fulfillment
of the Requirements
for the Degree of

Master of Science in
Chemical Engineering

Sharjah, United Arab Emirates

January 2016

Approval Signatures

We, the undersigned, approve the Master's Thesis of Najla Mohammad.

Thesis Title: Acoustically activated release of estrone-targeted liposomes used for breast cancer treatment.

Signature	**Date of Signature** (dd/mm/yyyy)
_____	_____
Dr. Ghaleb Al Husseini Professor, Department of Chemical Engineering Thesis Advisor	
_____	_____
Dr. Ana Martins Visiting Scholar, Department of Chemical Engineering Thesis Committee Member	
_____	_____
Dr. Rana Sabouni Assistant Professor, Department of Chemical Engineering Thesis Committee Member	
_____	_____
Dr. Naif Darwish Head, Department of Chemical Engineering	
_____	_____
Dr. Mohamed El-Tarhuni Associate Dean, College of Engineering	
_____	_____
Dr. Leland Blank Dean, College of Engineering	
_____	_____
Dr. Khaled Assaleh Interim Vice Provost for Research and Graduate Studies	

Acknowledgments

It is with sharing knowledge and experience that we learn, and with patience, dedication and motivation from kind people around us that we achieve our goals in life.

At this stage, I would like to take the opportunity to express my sincere gratitude to my thesis advisor Dr. Ghaleb Al Husseini for his direct supervision, precious comments and continuous support during the research.

I would like to deeply thank Dr. Rute Vitor from whom I learnt a lot in this research through her great efforts and assistance in the laboratory besides her generous encouragement.

I also thank the Department of Chemistry at the American University of Sharjah for giving us access to their research laboratory and facilities, and I take this opportunity to express my sincere gratitude to Dr. Mohammad Al Sayah who provided us with guidance and great insights during the entire phase of the laboratory work.

I am very grateful also to Dr. Ana Martins who provided assistance in writing this thesis through her valued comments and suggestions. And I sincerely thank my friend Salma Elgaili for enlightening my first steps in the research, and my teammate Renad Turki for her great support during the journey, and my colleague Hesham Gamal who contributed to this work.

My deepest gratitude I give to the faculty of the Department of Chemical Engineering at the American University of Sharjah who gave me the opportunity to pursue my dreams and goals in graduate studies though a teaching assistantship, and I also thank the head of the department Dr. Naif Darwish for his guidance and continuous support to all graduate teaching assistants during their study.

Last but not least, I want to warmly thank my family and friends who always support me, inspire me, and surround me with their kindness and love.

Dedication

I dedicate this work to my beloved parents who have always been in my side,

And to those who enlightened my mind.

Abstract

Chemotherapy is frequently used in cancer treatment. However, side effects associated with this type of treatment are often detrimental to the patient's health. This thesis discusses a novel approach of delivering a cytotoxic drug to tumor without affecting adjacent healthy tissues, thus minimizing the adverse side effects of conventional chemotherapy. Liposomes are nanocarriers used to encapsulate and deliver certain cytotoxic agents (e.g., doxorubicin) to malignant cells. Moieties can be attached to the liposome surface to target them to specific cancer cells, by interaction with specific cell membrane receptors. Once there, a stimulus, such as ultrasound can be used as a trigger to release the drug from these nanovehicles. In this study, estrone-targeted and non-targeted liposomes, encapsulating the model drug calcein, were synthesized. Estrone-targeted liposomes are promising delivery vehicles for breast cancer treatment, since most breast cancer cells overexpress receptors for this hormone. The sizes of the liposomes were determined by dynamic light scattering, and both were characterized as large unilamellar vesicles, with non-significant differences between them. The release from the synthesized liposomes triggered by ultrasound waves at low frequency (20 kHz) and high frequency (1.07 and 3.24 MHz), at several power densities, was determined by monitoring the changes in calcein fluorescence, using a spectrofluorometer. The final release at low frequency did not show a significant difference between both types of liposomes, when compared at the same power density, but the initial release rate, measured as the fluorescence increase after the first US pulses at 6.08 and 11.83 W/cm^2 power densities, was significantly higher for targeted liposomes. Increasing power densities showed a significant effect on release for both types of liposomes during the first two US pulses, but the final release for non-targeted liposomes showed a different response to power density as compared to targeted liposomes. Finally, the release for higher frequencies significantly increased with increasing power density, for both liposome type, but did not show a significant difference when both types were compared at the same power density and frequency.

Search Terms: *Drug delivery, ultrasound, liposomes, estrone, breast cancer, LFUS, HFUS.*

Table of Contents

Abstract 6

List of Figures 9

List of Tables 11

Nomenclature 12

Chapter 1: Introduction 13

Chapter 2: Literature Review 16

2.1. Drug Delivery System (DDS) 16

2.2. Liposomes 18

2.3. Methods for Liposome Preparation 20

2.3.1. Lipid film hydration method. 21

2.3.2. Reverse-phase evaporation (REV) liposomes. 22

2.4. Liposome Modifications 23

2.4.1. PEG coating. 23

2.4.2. Ligands and active targeting. 25

2.3.2.1. Estrogen hormones. 27

2.5. Ultrasound 30

2.5.1. Introduction to ultrasound. 30

2.5.2. Generation of ultrasound. 31

2.5.3. Physical properties of ultrasound. 32

2.5.3.1. Acoustic impedance. 33

2.5.3.2. Reflection of waves. 34

2.5.4. Ultrasound triggering. 35

2.6. *In vitro* Studies 37

2.7. *In vivo* Studies 38

2.8. Emulsion Liposomes (eLiposomes) 39

Chapter 3: Experimental Procedure 41

3.1. Materials 42
3.2. Preparation of DSPE-PEG-NH_2 and DSPE-PEG-$N_3C_3Cl_2$-ES Liposomes 42
3.2.1. Synthesis and IR analysis of estrone-$N_3C_3Cl_2$ chloride conjugate. 42
3.2.2. Synthesis of DSPE-PEG_{2000}-N_3C_3Cl-ES. 43
3.2.3. Preparation of DSPE-PEG_{2000}-N_3C_3Cl-ES liposomes encapsulating calcein. . 44
3.2.4. Preparation of DSPE-PEG_{2000}-NH_2 (control) liposomes encapsulating calcein. 45
3.3. Determination of Liposome Size by Dynamic Light Scattering (DLS) 45
3.4. Low Frequency Ultrasound Release Studies (Online Experiments) 45
3.5. High Frequency Ultrasound Release Studies (Offline Experiments) 46
3.6. Statistical Analysis 48
Chapter 4: Results and Discussion 49
4.1. Infrared Spectra of the ES-$N_3C_3Cl_2$ Conjugate 49
4.2. Particle Size Measurements by DLS 50
4.3. Low Frequency US-induced Release 50
4.3.1. DSPE-PEG_{2000}-NH_2 (control liposomes) 50
4.3.2. DSPE-PEG_{2000}- N_3C_3Cl-ES liposomes. 54
4.3.3. Comparison between ES-conjugated and control liposomes. 57
4.4. High Frequency US Release 60
4.4.1. DSPE-PEG_{2000}-NH_2 (control liposomes) 60
4.4.2. DSPE-PEG_{2000}- N_3C_3Cl-ES (targeted liposomes). 62
4.4.3. Comparison between ES-conjugated and control liposomes. 64
Chapter 5: Conclusion and Recommendations 66
References 68
Vita 76

List of Figures

Figure 1: Liposome constituents and configuration [27]. 19
Figure 2: Various structures and sizes of liposomes. Adapted from [27]. 20
Figure 3: Liposome preparation methods according to passive loading technique. Adapted from [31, 32]. 21
Figure 4: Different techniques to attach antibodies to liposome surfaces. (a) Surface absorption, (b) covalent coupling of the antibody, (c) PEG spacers, or (d) hapten binding, (e) and (g) Avidin-biotin with either avidin or biotin attached to the surface, (f) Fab'. Adapted from [42]. 26
Figure 5: Mechanisms of interaction between cells and liposomes. (a) Absorption, (b) fusion, (c) receptor-mediated endocytosis, (d) phagocytosis. Adapted from [42]. 27
Figure 6: Structure of human estrogen receptors ERα & ERβ. Adapted from [46]. 28
Figure 7: ER signaling mechanisms. (1) Classical mechanism of ER action, (2) ER-independent genomic mechanism, (3) Ligand-independent genomic mechanism, (4) non-genomic action [47]. 28
Figure 8: Estrone 2-D molecular structure. 30
Figure 9: Piezoelectric effect. (a) Polarized segment, (b) stretched segment and (c) compressed segment due to voltage difference imposed, voltage produced due to (d) compression and (e) tension applied on the segment. Adapted from [56]. 32
Figure 10: Synthesis of estrone-cyanuric derivative. 43
Figure 11: Synthesis of DSPE-PEG_{2000}-N_3C_3Cl-ES. 44
Figure 12: Online release experiment in a pulsed mode. 47
Figure 13: Fluorescence profiles for an offline experiment after 60 minutes of insonation with a 10-minute interval. 48
Figure 14: IR spectra of estrone and cyanuric chloride before the reaction (ES + $(NCCl)_3$) and the formed conjugate (ES-$N_3C_3Cl_2$) after the reaction. 49
Figure 15: Normalized release profiles for DSPE-PEG_{2000}-NH_2 liposomes triggered by 20-kHz LFUS at the power densities indicated in the legend. Results are average ± standard deviation of 2 liposome batches (3 replicates each). 51
Figure 16: Normalized release profiles for DSPE-PEG_{2000}-NH_2 liposomes triggered by 20-kHz LFUS at 6.08, 6.97, and 11.83 W/cm^2. Results are average ± standard deviation of 2 liposome batches (3 replicates each), and are shown for first two pulses in addition to final release. 52

Figure 17: Normalized calcein release profiles from DSPE-PEG_{2000}- N_3C_3Cl-ES liposomes triggered by 20-kHz LFUS at the power densities indicated in the legend. Results are average ± standard deviation of 2 liposome batches (3 replicates each)..... 55

Figure 18: Normalized release profiles for DSPE-PEG_{2000}-NH_2 liposomes triggered by 20-kHz LFUS at 6.08, 6.97, and 11.83 W/cm^2. Results are average ± standard deviation of 2 liposome batches (3 replicates each), and are shown for first two pulses in addition to final release. 55

Figure 19: Comparison of the normalized calcein release profiles from DSPE-PEG_{2000}- N_3C_3Cl-ES and DSPE-PEG_{2000}-NH_2 liposomes triggered by 20-kHz LFUS at (A) 6.08 W/cm^2, (B) 6.97 W/cm^2 and (C) 11.83 W/cm^2. Results are average ± standard deviation of 2 liposome batches (3 replicates each). 58

Figure 20: Comparison of calcein release from DSPE-PEG_{2000}-N_3C_3Cl-ES and DSPE-PEG_{2000}-NH_2 liposomes triggered by 20-kHz LFUS at the indicated power densities. (A) Release after the first US pulse, (B) release after the second US pulse, (C) final release. 59

Figure 21: Normalized calcein release profiles from DSPE-PEG_{2000}- NH_2 liposomes, triggered by 1.07 and 3.24-MHz HFUS, at the two power densities indicated in the legend. Results are average ± standard deviation of 2 liposome batches (3 replicates)..... 61

Figure 22: Normalized calcein release profiles from DSPE-PEG_{2000}-N_3C_3Cl-ES liposomes, triggered by 1.07 and 3.24-MHz HFUS, at the two power densities indicated in the legend. Results are average ± standard deviation of 2 liposome batches (3 replicates). 63

Figure 23: Comparison of the normalized calcein release profiles from DSPE-PEG_{2000}- N_3C_3Cl-ES and DSPE-PEG_{2000}-NH_2 liposomes triggered by 1.07 and 3.24-MHz HFUS, (◆) ES-1.07 MHz, 10.5 W/cm^2, (■) ES-1.07 MHz, 50.2 W/cm^2, (▲) ES-3.24 MHz, 173 W/cm^2, (◇) Control-1.07 MHz, 10.5 W/cm^2, (□) Control-1.07 MHz, 50.2 W/cm^2,(△) Control-3.24 MHz, 173 W/cm^2. Results are average ± standard deviation of 2 liposome batches..... 64

List of Tables

Table 1: Different sizes of liposomes [27]. 20
Table 2: Characteristic acoustic impedance for selected biological tissues [60]. 34
Table 3: Calcein release from DSPE-PEG_{2000}-NH_2 liposomes triggered by 20-kHz US at the indicated power densities. Results are average ± standard deviation of 2 liposome batches (3 replicates each). 52
Table 4: Calcein release from DSPE-PEG_{2000}- N_3C_3Cl-ES liposomes triggered by the 20-kHz probe at the indicated densities. Results are average ± standard deviation of 2 liposome batches (3 replicates each). 54
Table 5: Calcein release from DSPE-PEG_{2000}-NH_2 liposomes triggered by the 1.07 and 3.24-MHz probes at 10.5, 50.2, and 173 W/cm^2 power densities. Results are average of 2 liposome batches (3 replicates each)..... 61
Table 6: Calcein release of DSPE-PEG_{2000}- N_3C_3Cl-ES liposomes triggered by the 1.07 and 3.24-MHz probes at 10.5, 50.2, and 173 W/cm^2 power densities. Results are average of 2 liposome batches (3 replicates each)..... 64
Table 7: T-test with unequal variances including the p-values to compare calcein release from ES-conjugated versus control liposomes triggered by the 1.07 and 3.24-MHz probes at 10.5, 50.2, and 173 W/cm^2 power densities 65

Nomenclature

ABC-accelerated blood clearance
CLs-conventional liposomes
Cryo-TEM-cryogenic transmission electron microscopy
DDS-drug delivery systems
DLS-dynamic light scattering
DPPC-dipalmitoylphosphatidylcholine
DPPG-1,2-dipalmitoyl-*sn*-glycero-3-phosphoglycerol
DSPE-PEG$_{2000}$-Amine-1,2-distearoyl-*sn*-glycero-3-phosphoethanolamine-N-[amino(polyethylene glycol)-2000]
EPR-enhanced permeability and retention effect
ERα-estrogen receptor alpha
ERβ-estrogen receptor beta
EREs-estrogen response elements
ES-estrone
GFs-growth factors
HER2-human epidermal growth factor receptor 2
HIFU-high-intensity focused ultrasound
IgM-immunoglobulin M
LFUS-low frequency ultrasound
LUV- large unilamellar vesicles
LTSL-low temperature sensitive liposomes
MAb-monoclonal antibodies
MI-mechanical Index
MLVs-multilamellar vesicles
PC-phosphatidylcholine
PE-phosphatidylethanolamine
PEG-polyethylene glycol
PFC$_5$-perfluoropentane
PFC$_6$-perfluorohexane
PI-phosphatidylinositol
PS-phosphatidylserine
RES-reticuloendothelial system
SLs-stealth liposomes
TEA-triethylamine
TF-transcription factors
US-ultrasound

Chapter 1: Introduction

A recent study conducted by the American Cancer Society estimated the number of new cancer cases and cancer deaths in 2014 in the US as 1,665,540 and 585,720 for men and women, respectively (for all types of cancer, except basal cell and squamous cell skin cancers) [1]. According to these statistics, cancer is the second major cause of death in the US, following heart diseases [2].

Cancer is a disease caused by an abnormal, uncontrolled cell growth. Cancer, also known as a malignant tumor, is characterized by the fact that cells spread either by invasion or metastasis [3]. On the other hand, benign tumors are localized and less threatening than cancer. Normally, healthy cells follow a regular path of growth, division and apoptosis (programmed cell death) [4]. On the contrary, cancer cells do not undergo apoptosis, but they continuously keep growing and dividing due to DNA mutation that hinders the function of genes involved in cell division [4]. Genes responsible for cell division are of four types [3]:

i. Suicide Genes: control apoptosis.
ii. Oncogenes: determine when cells should divide.
iii. Tumor Suppressor Genes: regulate transcription, cell division, cell differentiation, and cell death.
iv. DNA-Repair Genes: repair damaged DNA.

Researchers in oncology invested great effort in understanding cancer and developing various treatments to minimize the number of deaths due to its being potentially fatal disease. Some of these treatments include surgery, chemotherapy, hyperthermia, radiation and targeted therapies [5]. Remarkable efforts have been made over the past century to make the treatment less painful and with fewer side effects. For example, in 1880s, Dr. William Halsted pioneered a surgical approach to treat breast cancer through radical mastectomy, which consists of the removal of the whole affected breast(s) with the surrounding lymph nodes and chest muscles [5]. After almost two decades, and in an attempt to approach a less invasive technique, radioactive materials were implanted close to the tumor site to treat it, a procedure termed “brachytherapy”. In 1971, another approach known as “total mastectomy” was implemented for early-stage breast cancer where the entire breast is removed excluding the muscle tissues and

lymph node. This last surgery is superior over the previous treatments since it involves less pain and is associated with the speedy recovery of the patient. It was also found that a combination of different modalities is beneficial. For instance, Drs. Fisher and Bonadonnav [5] found that adjuvant chemotherapy, an approach where chemotherapy is applied after a surgery, can prolong the lives of early-stage breast cancer patients up to five years. Finally, in 1998, the first targeted anti-breast cancer therapy, Herceptin, was approved as an adjuvant therapy for women diagnosed with early-stage HER2-positive breast cancer. Herceptin, a monoclonal antibody (MAb), was shown to reduce the recurrence of cancer by more than 50 % after two trials when it is added to chemotherapy [5]. Thus, targeted therapy has elevated the standard of care to a more advanced level with better relief and fewer detrimental side effects.

Chemotherapy can treat many types of cancer, since it consists of antineoplastic agents of different classes and modes of action [6]. Chemotherapy targets fast growing cells including tumor cells, hair follicles, cells lining the mouth and digestive track [7]. Thus, some of the side effects of chemotherapy are hair loss and diarrhea. Cytotoxic agents do not distinguish between normal cells and malignant cells, affecting both equally, leading to various side effects including nausea, vomiting, fatigue and appetite loss [6, 8]. Therefore, researchers developed an innovative approach to make the treatment more targeted and less invasive - the so-called "targeted therapies." These therapies are intended to attack a specific target in the cell which inhibits the growth pathways [4]. Targeted therapies are classified into therapeutic monoclonal antibodies and small molecules [9]. Therapeutic monoclonal antibodies are more targeted than small molecules, since they bind to particular antigens located on the surface of the cell. Additionally, antibody-based drugs have a long half-life (2-3 weeks) which allows them to treat chronic diseases. The mechanism of targeted therapies is based on the blockage of the growth factor receptors, and hence blocking the signals responsible for cancer growth [4]. Also, researchers found that nanoscale therapeutic carriers can be combined with ultrasound (US) as a triggering technique, to deliver cytotoxic agents to specific tissues or cells using an appropriate ultrasonic frequency, power density and other acoustic factors [10]. The technique of using nanocarriers in conjunction with a trigger, known as a drug delivery system (DDS), can enhance pharmacological properties by modifying drug pharmacokinetics and biodistribution [11]. The nanoparticles used in DDS include micelles, liposomes, dendrimers and other polymeric-based systems [11].

In this work, estrone-anchored liposomes were synthesized and studied, as part of a strategy to target breast cancer cells that overexpress estrogen receptors (ERs). Estrone is a steroidal hormone with various functionalities. Research has shown that almost two-thirds of breast cancer overexpress estrogen receptors [12]. Additionally, it has been reported that the binding of estrogen hormones to their receptors in cancer cells increases cell division and leads to DNA mutation [13]. And in order to achieve the aim of this thesis, the following tasks will be performed:

1) The synthesis of estrone-cyanuric anchored stealth liposomes.
2) The synthesis of control liposomes (i.e., non-targeted liposomes).
3) The characterization of targeted and non-targeted liposomes.
4) The evaluation of the acoustic calcein release from the aforementioned types of liposomes, triggered by 20 kHz-LFUS at the following power densities: 6.08, 6.97, and 11.83 W/cm^2.
5) The evaluation of the acoustic calcein release from the mentioned liposomes at 1.07- and 3.24-MHz HFUS and the following power densities: 10.5 and 50.2 W/cm^2 at 1.07 MHz and ~173 W/cm^2 at 3.24 MHz.

Chapter 2: Literature Review

2.1. Drug Delivery System (DDS)

Chemotherapeutic agents can suppress tumor growth. However, they target both normal and cancer cells. Also, the dose of chemotherapy is critical and bound by two levels, known as therapeutic indices: the maximum level for which the patient experiences undesirable effects if exceeded, and the minimum level where the drug efficiency is not attained [14]. Therefore, the drug should be delivered with a dose between the two levels and, in order to achieve this, researchers developed carriers as a part of DDS to deliver a desirable dose to target specific cells in order to reduce unintended side effects of regular chemotherapy, and to deliver a therapeutic amount of drug. Additionally, these carriers retain the bioavailability of the drug. Drug delivery systems are classified into four categories, based on their functional mechanism: diffusion-controlled, chemically-controlled, water penetration-controlled and response-controlled [14]. The latter is marked as "smart DDS" since the mechanism is based on the sensitivity of the carrier to internal or external stimuli in the surrounding environment such as temperature, pH, ionic strength, ultrasonic waves, electric field, etc. [14].

Different nanoparticles are used in DDS. Many factors affect their ability to move within and interact with the surrounding environment, including size, shape, charge, coating, cargo and material [15]. The size of a nanoparticle affects the circulation time, extravasation, interstitial diffusion and the ability to be internalized by the cell. Small nanoparticles of 5 nm or less can escape the bloodstream easily to penetrate the adjacent tissues. They are also rapidly filtered by kidneys. The latter action results in a short circulation time that is often in the order of a few minutes. Although small nanoparticles diffuse easily into tumor tissues, sometimes these particles are repelled by the tumor due to the hydrostatic pressure gradient that is part of the tumor physiology. Larger nanoparticles (5 nm to 500 nm) have better circulation time and can diffuse into the tumor site via pores and defects in angiogenic vessels [15]. The shape of a nanocarrier significantly contributes to its biodistribution, cellular uptake and the passage through the reticulo-endothelial system (RES) [16, 17], and it also affects the propensity of a particle to phagocytosis, thus affecting circulation time [16]. For instance, filamentous micelles, around 18 μm in length and 20 to 60 nm in diameter, were observed to be retained in circulation for one week, compared to spherical

PEGylated stealth vesicles which were cleared within two days by the RES [16, 17]. Also, the shape of a nanoparticle can affect the drug bioavailability inside tumor. This was observed for worm-like iron oxide nanoparticles that accumulate more inside the tumor compared to nanospherical particles [16]. Fox *et al.* [18] suggested that the entry and the passage of polymeric drug carriers with approximately similar volumes through the pores are also affected by the particle shape and flexibility. Researchers found that this affects the renal clearance of the nanocarrier, thus influencing both the circulation time and biodistribution [16]. As an example, linear polymers have loose random coil conformations in solution which enable them to easily enter through pores by one end of the chain. On the other hand, cyclic polymers exhibit a deformation while entering and passing through a pore due to the lack of chain ends making their route harder.

Based on clinical trials, liposomes and micelles proved to be the most efficient nanocarriers for chemotherapeutic delivery. Vesicles with small size (~100 nm or less) can extravasate from circulation through defects and vascular gaps into tumors due to angiogenesis [11]. It is observed that the rate of angiogenesis in tumors occurs in a fast rate compared to other normal cells, except for vessels formed while healing wounds or those during pregnancy [19]. Additionally, the retention time of these nanocarriers in tumor sites is high due to poor lymphatic drainage in tumors [11]. On the other hand, the lower size limit of 20 nm (in diameter) of these carriers protects normal cells from being attacked by the chemotherapeutic drug [11].

Apart from the benefits of drug delivery vehicles, some difficulties may limit their efficiency. One of these limitations is the low bioavailability due to opsonization. Foreign bodies, such as nanocarriers, are marked for removal by RES organs resulting in their poor accumulation inside tumors [11]. To solve this issue, researchers found that the circulation time of nanocarriers *in vivo* can be enhanced by coating them with polymers such as polyethylene glycol (PEG), which are capable of delaying their clearance from circulation [11, 20]. The improvement of the nanocarrier circulation by PEG coating, along with the tumor features of low lymphatic drainage and porous angiogenic endothelium, is responsible for a phenomenon called the *enhanced permeability and retention* effect (EPR) [11]. Additionally, "PEG-lipids" are safe to use in the body since they are water-soluble and biocompatible [11]. However, although PEG may enhance the pharmacokinetics of the drug and the stability of the nanocarriers

in circulation, it may reduce the tumor uptake, since PEG molecules pose a steric barrier between the carrier and the tumor cells [11, 21]. The mentioned nanocarriers so far are under the *passive targeting*, since these vesicles depend on their leakage into the tumor site followed by the cellular uptake of the drug [11]. Thus, researchers invested considerable efforts to make the drug delivery more selective using *active targeting*. The basic mechanism of active targeting is either to improve the co-localization of the drug and cancer cells [22], or to improve the cellular internalization via receptor-mediated endocytosis by attaching ligands to the surface of the nanocarriers [11]. Ligands are defined as molecules that can effectively guide therapies to specific cell biomarkers to achieve certain functionality [23]. The ligands attached to the nanocarriers are chosen, so they can identify specific receptors on the surface of the targeted cells, and selectively bind these receptors [11].

2.2. Liposomes

Liposomes are widely used in drug delivery. The Greek root of the word 'liposome' means "fat body". To describe it further, a liposome is defined as a hollow structure made of a phospholipid bilayer, similar to the membrane of animal cells. Liposomes were first discovered in 1960s by the British scientist Alec Bangham, when studying the effect of phospholipids on clotting blood [24]. Bangham noticed that spherical structures formed when adding water to a phospholipid film, thus encapsulating part of the liquid medium. Afterwards, this great discovery triggered further research on the uses of liposomes in various applications, including gene and drug delivery, dye delivery to textiles, pesticides delivery to plants, enzymes and nutrition delivery to foods, and transformation of DNA to host cells [24, 25]. Liposomes are biocompatible and biodegradable in nature and, due to their amphiphilic nature, they can be loaded with hydrophobic drugs in their lipid bilayer, and with hydrophilic drugs in their inner core [26].

The main constituent of liposomes are phospholipids [16] which are tadpole-like molecules that consist of a hydrophilic head attached to a nonpolar fatty-acid hydrophobic tail, refer to Figure 1 [24, 27].

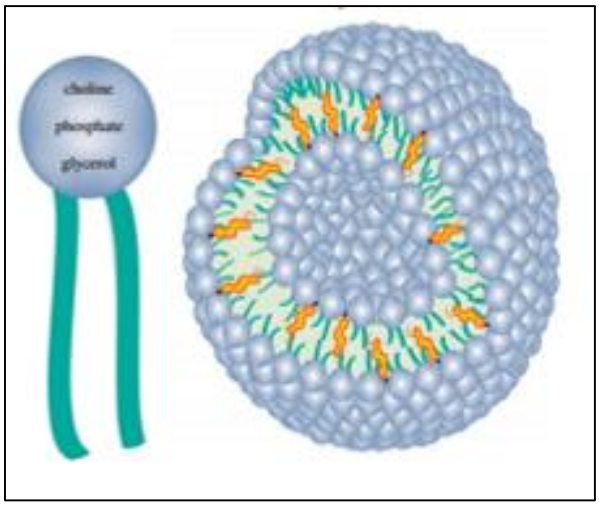

Figure 1: Liposome constituents and configuration [27]**.**

The polar head of a phospholipid molecule consists of glycerol and a modified phosphate group while the nonpolar tail consists of two long hydrocarbon chains [24]. Phospholipid head groups found in nature usually contain phosphatidylcholine (PC), phosphatidylethanolamine (PE), phosphatidylinositol (PI), and phosphatidylserine (PS). Common natural sources for phospholipids are soya bean or egg yolk, but neither can be used in clinical applications due to stability and contamination issues [27]. Synthetic phospholipid derivatives include, but are not limited to, 1,2 dipalmitoyl-*sn*-glycero-3-phosphoglycerol (DPPG), dipalmitoylphosphatidylcholine (DPPC), and hydrogenated soy phosphatidylcholine (HSPC). Due to the amphiphilic (exhibiting both hydrophobic and hydrophilic behavior) nature of phospholipid molecules in water, they tend to form a bilayer sheet structure, with the phospholipid heads oriented outwards the aqueous medium, while sequestering all the nonpolar tails from any contact with this medium [24]. Cholesterol is another constituent of liposomes, and cell membranes. It is embedded in liposomes to increase their stability by modulating the fluidity of the lipid bilayer and preventing crystallization of the phospholipids acyl chains [28]. When cholesterol is added to unsaturated lipids, their permeability to water decreases [27]. Hence, liposomes with a high percentage of unsaturated fatty acids can hold water-soluble drugs more efficiently if cholesterol is added, providing a better encapsulation. Also, since steroid rings of cholesterol are dense, their presence increases the mechanical rigidity of the lipid bilayer.

Liposomes are classified on the basis of lipid bilayer into small unilamellar vesicles (SUVs), multilamellar vesicles (MLVs) and multi-vesicular vesicles (MVVs),

see Figure 2. Additionally, they are classified on the basis of size into small unilamellar vesicles (SUVs) and large unilamellar vesicles (LUVs), see Table 1.

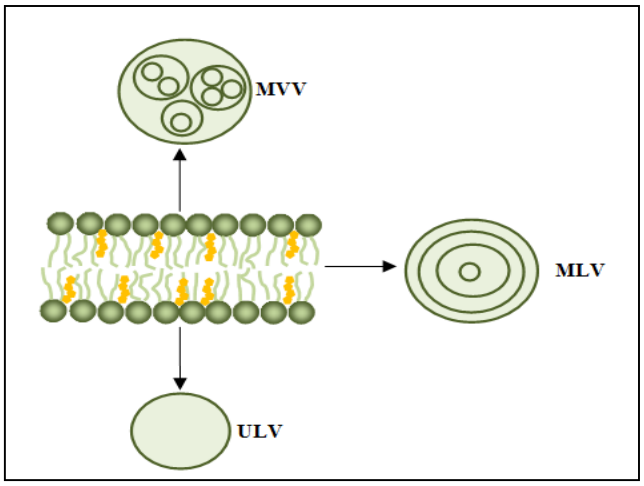

Figure 2: Various structures and sizes of liposomes. Adapted from [27].

Table 1: Different sizes of liposomes [27].

Type of Liposome	Size (in diameter)
MVVs	1.6-10.5 µm
MLVs	0.1-15 µm
ULVs LUVs SUVs	 100 nm-1 µm 25-50 nm

2.3. Methods for Liposome Preparation

Liposomes have a vital role in drug delivery, and thus many researchers have been developing various techniques to prepare liposomes with certain characteristics. In general, drug is loaded in liposomes either by passive or active methods [29]. According to Cullis *et al.* [30], the main variables to be considered in drug encapsulation are trapping efficiency, drug retention and drug-to-lipid ratio. According to the author, trapping efficiency favors procedures that achieve high drug encapsulation (> 90%), while drug retention is significant for storage purposes and drug release during treatment. Passive loading includes techniques where drug and lipids are both dispersed in an aqueous buffer, hence drug entrapment occurs during liposome preparation. On the other hand, active loading methods involve drug encapsulation, after forming liposomes, by establishing membrane potential or transmembrane pH. The choice of the liposome preparation method depends on many factors including [31]:

i. The medium used to disperse lipids.
ii. The characteristics of the substance to be entrapped and of the constituents used in the liposome formulation.
iii. The concentration of the substance to be encapsulated.
iv. The physical properties of liposomes such as: size, polydispersity, and the shelf-life of vesicles.

In general, liposomes are classified into three main categories, according to their method of preparation: (i) mechanical dispersion, (ii) solvent dispersion, and (iii) detergent removal, refer to Figure 3 [31]. A few of these methods will be further discussed in the following sections.

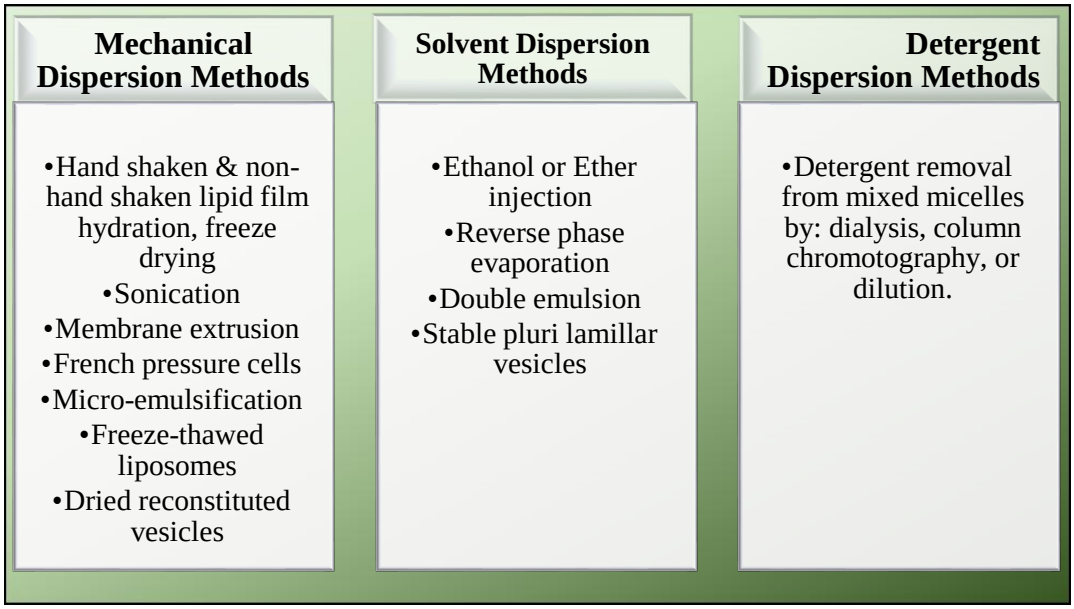

Figure 3: Liposome preparation methods according to passive loading technique. Adapted from [31, 32].

2.3.1. Lipid film hydration method.

To prepare liposomes according to the lipid film hydration method, the lipids are first dissolved in an organic solvent or mixture of organic solvents (e.g., chloroform or chloroform/methanol 2:1 (v/v)) in a round bottom flask or vial, to obtain a homogenous mixture with a concentration of 10-20 mg lipids/ml of solvent [31, 33]. Then, the organic solvent can be evaporated by purging the sample with nitrogen or argon when the volume of the solvent is small (<1 ml), or by using a rotary evaporator for larger samples [31]. The drying is performed at a temperature above the phase transition temperature (T_m) of the lipids [33]. The lipid film is then hydrated with an aqueous medium at a

temperature above the T_m, by placing the round bottom flask into a hot bath using a rotary evaporator without vacuum up to one hour [31, 33]. If the film is not fully dissolved, more agitation is required. The hydration media may be distilled water, or buffered solution or saline. The product of this synthesis includes a mixture of milky-like multilamellar large vesicles (MLVs) [33].

To downsize the MLVs into small unilamellar vesicles (SUVs), various techniques are available with sonication being one of the most widely used mechanical methods. To sonicate the sample of MLVs, either a beaker containing the sample is placed in a sonicating bath, or a sonicator probe is immersed into a tube containing the suspension. In the latter case, the temperature of the sample should be carefully controlled not to exceed the transition temperature, because the sonicator tip delivers a very high energy into the sample, which may induce local heating that can de-esterify the lipids if sonicated for one hour [33]. Moreover, probe-tip sonicators were found to contaminate the sample with metals (e.g., titanium) that can be removed by centrifugation [31, 33]. For these reasons, bath sonicators are preferably used. The temperature of the bath should be above the T_m of the lipids, and usually sonication is performed for 10-15 minutes. During sonication, the suspension will convert from a milky-like to an opalescent solution. Vesicles with small diameter (<40 nm) produced after sonication are metastable, i.e. due to the high curvature energy they tend to fuse with others to form bigger vesicles (d= 60-80 nm) that are more stable [33].

2.3.2. Reverse-phase evaporation (REV) liposomes.

The REV method, introduced by Szoka and Papahadjopoulos in 1978 [34], was one of the most significant achievements in liposome preparation. At the time of its implementation, this was the first technique allowing for high encapsulation efficiency of aqueous medium [33]. Additionally, REV is applicable for various lipids, including cholesterol, and can achieve an aqueous volume-to-lipids ratio up to 30 times of that obtained from SUVs prepared by sonication and four times of MLVs achieved by lipid film hydration method [33]. The major drawback of the REV rises when proteins are to be encapsulated, due to the possible denaturation of the latter upon mixing with an organic medium [33, 34]. It is also important to mention that encapsulation efficiency varies among different types and concentrations of lipids, and is dependent on the ratio of lipids-to-organic solvent-to-buffer.

The protocol for REV includes, in its initial step, the formation of inverted micelles by sonication according to Torchilin and Weissig [33]. The synthesis starts with the solution of lipids in chloroform which is dried in a rotary evaporator. Then, the lipids are dissolved in an organic phase such as diethyl ether, followed by the addition of an aqueous medium containing the molecules to be encapsulated, in a ratio 3:1 (v/v) organic phase-to-aqueous medium, which is required to achieve an optimum encapsulation efficiency. To form inverted micelles, the two-phase solution is then sonicated 2 - 5 min in a sonicating bath, at a temperature below 10 ^{o}C to avoid the separation of dispersed micelles from the organic phase, until the mixture becomes an opalescent one-phase solution. After sonication, diethyl ether is evaporated at room temperature under reduced pressure in the rotary evaporator. During evaporation, it is important to avoid foam formation and if any sign of bubble formation appears, the pressure should be raised immediately. After evaporation, inverted micelles become viscous and some of them will disintegrate to build up a second layer around the remaining inverted micelles to form what is known as REV liposomes. Liposomes formed using this method are mostly unilamellar with heterogeneous size distribution (100 nm - 1 μm), and they can be purified by centrifugation or by size-exclusion chromatography using a Sepharose 4B column.

2.4. Liposome Modifications

2.4.1. PEG coating.

Liposomes provide a good encapsulation technique for drugs, hence reducing drug degradation. Liposomes were observed to target tissues and organs with discontinuous endothelium, such as the liver, spleen and bone marrow [35]. Similarly, these nanoparticles can also target tumor tissues due to the presence of a discontinuous endothelium. The accumulation of liposomes in the tumor site by passive targeting is commonly known as the EPR effect, as mentioned before. On the other hand, liposomes cannot extravasate from the bloodstream into normal tissues because these have tight junctions between capillary endothelial cells. It is important to note that the *in vivo* response to the EPR effect was found to be greater than that evaluated clinically as reported by Nicholas and Bai [36]. This is justified by tumor irregular vascular distribution and pressure imposed by internal fluids [19, 36]. Upon intravenous administration, liposomes are captured immediately by the RES and cleared from the blood circulation [35]. The first step of recognizing liposomes is the binding of selected

serum proteins (opsonins, such as fibronectin and immunoglobulins) which triggers the RES to identify them. This liposome capture by the RES is advantageous to treat RES-related infections, such as leishmaniasis, by delivering antiparasitic and antimicrobial drugs. However, when liposomes are utilized to deliver drugs to other tissues, their uptake by macrophages is considered a major drawback. Therefore, there was a need to design liposomes with prolonged blood circulation. Immordino *et al.* [35] found that coating liposomes with hydrophilic polymers, such as PEG, isolated them from macromolecules such as opsonins and other proteins, thus reducing the interaction between liposomes and macrophages, and allowing an increased circulation period. PEGylated liposomes are also known as *stealth* liposomes or *sterically stabilized* liposomes (SLs), as opposed to conventional liposomes (CLs) (without PEG coating). Stewart *et al*. [37] reported a median circulation half-life of 55 hours for stealth liposomes in plasma compared to a 6-hour half-life for conventional liposomes. Coating liposomes with PEG basically creates a steric stabilization which repels other plasma molecules. The use of PEG has many advantages: it is non-toxic, biocompatible and soluble in aqueous medium [35]. The modification of the liposomes' surface by PEG can be achieved in many ways: through physical adsorption, by incorporating PEG-lipid conjugate during liposome preparation, or by covalently attaching reactive groups to the surface of the liposomes. Poly(ethylene) glycol not only reduces the uptake of liposomes by macrophages, but it also enhances the stability of liposomes by reducing aggregation. For liposomes composed of phospholipids and cholesterol, the ability to increase the circulation time by PEG depends mainly on the amount of grafted PEG and the length, or equivalently, the molecular weight of the polymer. It was observed that long chains of PEG reflected an increase in circulation time, as reported by Allen *et al*. [38]. Additional research aimed to attach PEG to the liposomal surface, but in a reversible manner, in order to improve the continuous capture of liposomes by the cells. In this case, the fact that tumor sites have a lower pH, was used to detach the PEG coating once liposomes accumulate in the tumor [35]. One major limitation of using both conventional and stealth liposomes is observed after the first dose of treatment. Wang *et al.* [39] observed that a second dose of stealth liposomes, injected a few days after the first dose, possessed a decreased circulation time and instead, liposomes accumulated in the liver, despite the presence of PEG. This phenomenon is known as "accelerated blood clearance (ABC)," and is initiated by the production of anti-PEG Immunoglobulin M

(IgM) in the spleen, as a response to an injected dose of stealth liposomes [39]. Anti-PEG IgM binds to PEG and activates the complement system to opsonize liposomes which are captured in Kupffer cells in liver. Interestingly, the ABC phenomenon was also observed when the first dose is composed of conventional liposomes, followed by a second dose of stealth liposomes, but not conventional ones according to the author. These findings raise a major concern regarding the use of liposomes in clinical applications. Researchers found a correlation between the ABC effect and other factors such as the type and the amount of the initial dose, the interval between injections, the surface density of grafted PEG, and the surface charge of the nanocarrier. Ishida and Kiwada [40] found that the ABC phenomenon is inversely related to the initial amount of the PEGylated liposomes administered. Wang *et al.* [41] found that the ABC phenomenon only slightly occurred when a first dose of 110 nm conventional liposomes (i.e., without PEG) was injected into a rat, regardless of the charge of liposomes. On the other hand, the administration of smaller liposomes (60 nm) reflected an increase in the ABC phenomenon. More details about the factors interfering with the ABC phenomenon can be found in Ishida and Kiwada [40] and Wang *et al.* [41] research.

2.4.2. Ligands and active targeting.

Cancer cells usually overexpress certain receptors such as epidermal growth factor, folate, transferrin, fucose and estrogen receptors. To use liposomes in active targeting, targeting moieties are attached to the surface of liposomes. These moieties, such as monoclonal antibodies (MAb), fragments of proteins, peptides, carbohydrates and other receptor ligands, allow specific targeting for certain receptors on the surface of cells [35]. Targeting drugs is a beneficial process, since the cytotoxic agent is delivered to specific tissues, thus reducing the adverse side effects of conventional chemotherapy. A large number of ligands can be attached to the liposomal surface allowing for multivalency that achieves high avidities using ligands of low individual affinities [42]. Ligands may also increase the uptake of liposomes by the liver and spleen even in the presence of PEG [43]. Therefore, researchers found that a lower surface density of ligands is a critical factor in binding the liposome to the desired target, while maintaining a prolonged circulation [43].

Antibodies are among the most widely used ligands attached to liposomes surfaces, creating what are commonly known as *immunoliposomes*. The use of

antibodies has advantages over the use of peptides, due to their high affinity and specificity for a wide range of antigenic determinants, while maintaining a uniform structure, their biocompatibility and their well-established chemistry [42]. There are different ways to bind ligands to liposomal surfaces, e.g. surface adsorption and covalent coupling, see Figure 4. The location where the ligands are attached is also critical. Studies conducted by Maruyama *et al*. [44] aimed to investigate the effect of attaching monoclonal antibodies or their fragments to different positions in stealth liposomes. They reported that antibodies, bound directly to the liposome surface adjacent to PEG, showed lower targeting to mouse pulmonary endothelial cells than those attached to PEG terminal ends.

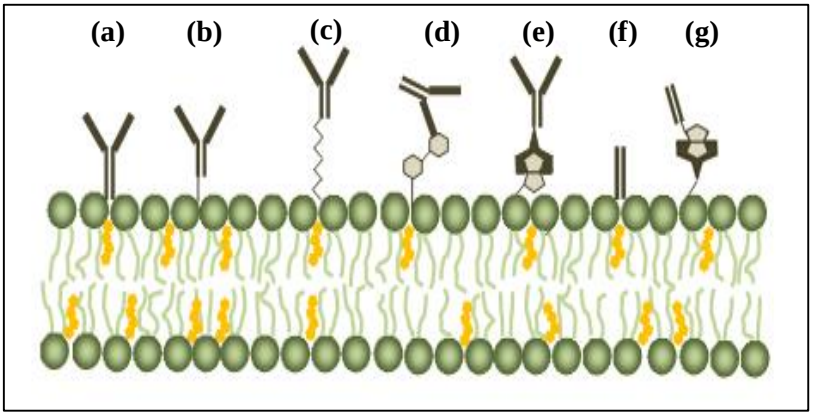

Figure 4: Different techniques to attach antibodies to liposome surfaces. (a) Surface absorption, (b) covalent coupling of the antibody, (c) PEG spacers, or (d) hapten binding, (e) and (g) Avidin-biotin with either avidin or biotin attached to the surface, (f) Fab'. Adapted from [42].

After making the nanocarrier selective by attaching a targeting moiety, a biological mechanism is needed to deliver the encapsulated drug into the tumor site. Liposomes can deliver their content to cells through various mechanisms including membrane fusion, endocytosis and extracellular release [42]. These mechanisms are depicted in Figure 5. In mechanism (a), liposomes release their content after surface absorption, so that free drug is absorbed by the cell. In mechanism (b), liposomes fuse with the cell membrane to deliver their content. Mechanism (c) represents receptor-mediated endocytosis, where liposomes less than 150 nm in diameter are attached to the cell surface receptors, and then drawn into clathrin-coated pits to form coated vesicles. These vesicles diminish later and liposomes are fused with lysosomes where lipids are degraded and drug is released. For molecules larger than 150 nm, phagocytosis (pino-cytosis) in mechanism (d) is followed [42].

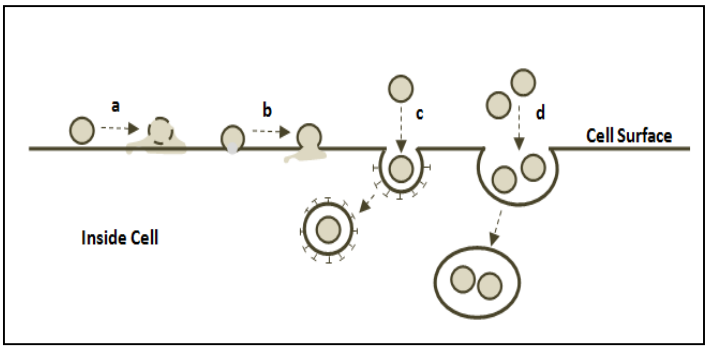

Figure 5: Mechanisms of interaction between cells and liposomes. (a) Absorption, (b) fusion, (c) receptor-mediated endocytosis, (d) phagocytosis. Adapted from [42].

2.3.2.1. Estrogen hormones.

Some ligands are classified as endogenous ligands, also known as bio-self molecules. These ligands, including antibodies, polypeptides, hormones and fusogenic proteins, have the advantage of being non-immunogenic and biocompatible [13]. Some of the receptors binding to endogenous ligands are transferrin receptors, lipoprotein receptors, hormone receptors, and receptors present on tumor cells. Estrogens, sex hormones that have a crucial role in the development of reproductive organs, are one of the important steroid hormones that work as chemical messengers in the body. Estrogens include estrone, estradiol and estriol, which are primarily produced in ovaries, specifically from testosterone and androstenedione, and are secondarily produced in adrenal cortex, testes and placenta. Estradiol is the main form of estrogen during reproductive years, while in menopause, estrone is the main estrogen in the body. The third estrogen, estriol, is predominant during pregnancy [45]. Estrogens are also important in the regulation of the urinary tract, bones, heart and blood vessels, breast, skin and hair. Estradiol is the most potent estrogen due to its high affinity in receptor-ligand interaction. In the reproductive system, estrogens support the development of female breast tissues, while in the cardiovascular system, they play a role in lowering the concentration of lipids that affect blood vessels, and also increase the blood flow in vessels and decrease the vascular resistance. Estrogens are also biologically produced in the brain and body fat, thus interfering with several functions in the nervous system such as memory, temperature regulation and awareness. The function of estrogen is mainly mediated by two receptor proteins: the estrogen receptor alpha (ERα) and beta (ERβ) [13]. Estrogen receptors (ERs) consist of a single polypeptide chain that contains six functional domains, see Figure 6. The molecular weights for human ERα and ERβ are 66 kDa and 54 kDa, respectively [46]. The percentage of homology between each of the

functional groups in ERα and ERβ is shown in Figure 6. Domain C, which shows the highest similarity between receptors, includes two zinc fingers that bind hormone elements responsible for DNA interactions. On the other hand, the N-terminal domain (A/B) shows the least percentage of homology and includes the ligand-independent-transcriptional-activation function TAF-1. The D-domain is a hinge region, while the E-domain includes the hormone binding domain and the hormone-dependent-transcriptional-activation function TAF-2 [46].

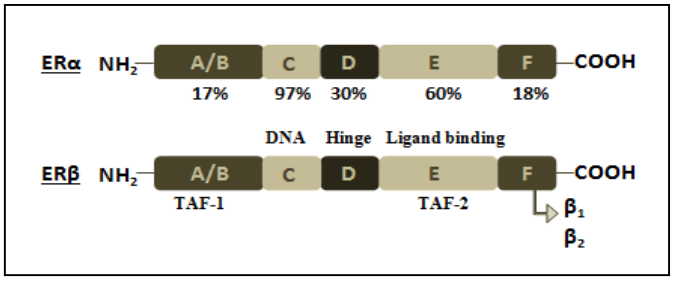

Figure 6: Structure of human estrogen receptors ERα & ERβ. Adapted from [46].

In addition to the reproductive system, estrogen receptors are expressed in other organs/systems such as the liver, cardiovascular system, bones and breasts. ERα is overexpressed in breast cancer cells, stromal compartment of prostate and ovarian stroma cells [13]. Thus, estrogen ligands can be used in drug delivery to target cancer cells via estrogen ligand-receptor interaction. ERβ is expressed in the central nervous, cardiovascular, immune and reproductive systems [13]. Steroid hormones are lipophilic, which allows them to pass through the cellular membrane by passive diffusion and bind to their corresponding receptors that are located either in the nucleus or in the cytoplasm and sometimes on the exterior membrane of the cell. Several mechanisms are reported for estrogen-receptor binding interaction, as shown in Figure 7.

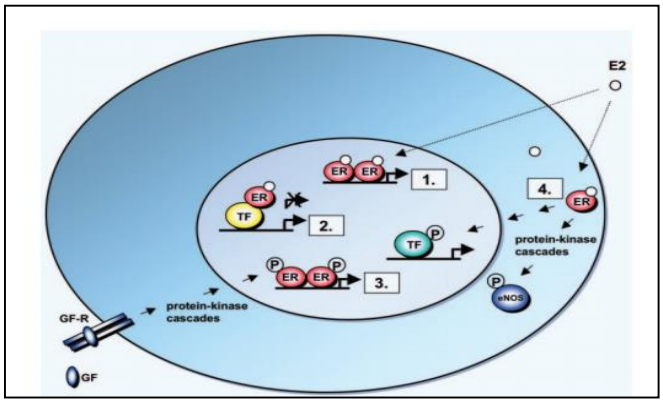

Figure 7: ER signaling mechanisms. (1) Classical mechanism of ER action, (2) ER-independent genomic mechanism, (3) Ligand-independent genomic mechanism, (4) non-genomic action [47].

First, the classical mechanism involves the direct binding of estrogen to its corresponding receptor in the nucleus. This causes the receptor to dimerize and bind to estrogen response elements (EREs) that are located on the target genes. However, it has been found that one-third of the human genes that are regulated by estrogen receptors lack the ERE sequence, suggesting that additional mechanisms are needed to regulate gene expression [47]. Second, the ER-independent genomic mechanism controls the gene expression by regulating transcription factors through protein-protein interaction instead of directly binding to DNA; this mechanism is often used to regulate genes lacking the ERE sequence. Third, the ligand-independent genomic mechanism includes growth factors (GFs) that activate the protein-kinase cascades. This leads to the phosphorylation (P) and subsequent activation of ERs at the ERE sequences on the genes. The last mechanism is characterized as non-genomic, which usually occurs faster than the genomic ones; in this case the estrogen-ER complex phosphorylation (P) targets proteins, which activates their function in the cytoplasm or triggers the action of transcription factors (TF) in the nucleus.

In 1896, Beatson announced the dependence of breast cancer on hormones, namely estrogens, and two different hypotheses have been formulated to explain the role of estrogen in breast cancer development [13]. The first hypothesis suggests the proliferation of mammary cells after the binding of estrogen to its receptor, which results in an increase in cell division and DNA replication that ultimately leads to lethal mutation. The second hypothesis considers a point mutation as a result of DNA damage caused by side products of estrogen metabolism. In both cases, there is a disturbance of apoptosis and DNA-repair mechanisms, leading to tumor development [13].

Estrogen receptors are present in two-thirds of breast cancer and they are distributed in the nucleus and on the cell membrane [12]. The presence of ERs on the cell membrane can be utilized in guiding therapies towards breast cancer cells [12]. In postmenopausal women, the major estrogen is estrone which is primarily produced from the aromatization of androstenedione, which is mainly (~ 95%) produced in the adrenal glands [48]. Estrone has the second highest affinity to ER after estradiol. It transfers the majority of its signal (60%) to ERα while 37% of its signal is transferred to ERβ [49]. Since breast cancer overexpresses ERα, estrone is considered as a potential ligand in cancer therapeutic drugs especially for postmenopausal women. Estrone has a molecular weight of 270.4 g/mol and its chemical formula is $C_{18}H_{22}O_2$ with a chemical name of 3-

hydroxyestra-1,3,5(10)-triene-17-one [50]. The 2-D molecular structure of estrone is shown in Figure 8.

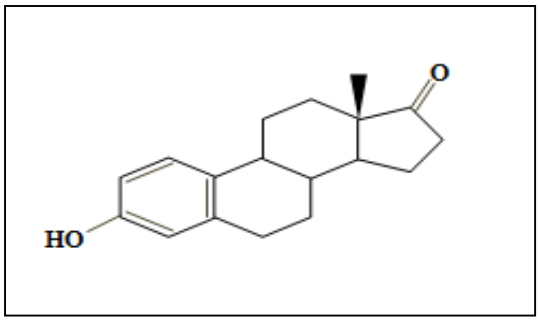

Figure 8: Estrone 2-D molecular structure.

2.5. Ultrasound

2.5.1. Introduction to ultrasound.

Ultrasound is composed of oscillatory sound pressure waves with frequencies higher than the audible limit of humans (i.e., >20 kHz) [51]. Pressure waves, known also as stress waves, require a medium to propagate because their transmission occurs by direct contact of masses [52]. Additionally, these waves depend on the elasticity nature of the medium, which plays a key role in sustained vibrations, hence stress waves are also known as elastic waves [51]. These waves can be induced by vibrating piezoelectric transducers. They became a prominent topic in research since World War I (1918) when a French scientist, Paul Langevin, developed the quartz ultrasonic transducer [53]. Many scientists, from different disciplines, have contributed to the development of acoustics science. For example, Sir Isaac Newton (1642-1727) derived the velocity of the sound wave in air; Jean Fourier (1768-1830) introduced mathematical series that have been used to study ultrasonic waves; and it was the observation of the Italian biologist Lazzaro Spallanzani (1729-1799) that triggered the idea of SONAR when he discovered that bats used US to navigate in the dark. The thorough research in acoustics, accompanied by the technological advancements and the progress in theoretical analysis and computer modeling in the 1970s, allowed the subsequent use of US in a wide range of fields, such as aerospace, defense, nuclear, engineering, materials science, metrology, biology and chemistry.

Ultrasound waves can be classified, according to their intensities, into low-intensity and high-intensity waves, which have different applications. For example, applications like nondestructive characterization of materials, medical diagnosis and the

area of sensors, which only require the transmission of energy through a medium without changing it, use low-intensity US [51]. On the contrary, when US waves are meant to cause/ impose an effect on the medium being propagated through, the suitable choice is to use waves with high intensity. Ultrasound waves with high intensity are often associated with thermal or mechanical effects which can be used to induce cavitation events. These are usually applied, for example, in kidney stone shattering, tumor ablation, cell lysis, emulsification, atomization of liquids and welding plastics or metals [51, 52]. Drug delivery is an evolving area of research. This paper will focus on US as a triggering mechanism by inducing mechanical and/or thermal effects on nanocarriers. A more detailed discussion on US nature and properties will be introduced in the following sections.

2.5.2. Generation of ultrasound.

Ultrasound waves can be generated in three ways: the Galton's whistle, the magnetostriction, and the piezoelectric method [54]. Francis Galton invented a special type of whistle that generates US waves that can be used to train animals. Such whistles are capable of producing sound waves with frequencies up to 30 kHz [54]. Magnetostriction, a phenomenon utilized to generate US, was first discovered by Joule in 1847. Joule describes magnetostriction as a change in the dimensions of a ferromagnetic material (e.g., iron, nickel) with a rectangular-bar shape when a magnetic field is applied along its axis [55]. If the field is non-oscillating, it will result in a minor increase in the bar length (10^{-6} of the original length for a nickel bar) [55]. However, when an oscillating field is applied, it will cause a significant increase in the bar length since the elasticity of the material can no longer counteract the change imposed. Usually, magnetostriction is used to generate US with a maximum frequency of 2 MHz, thus another method is required to generate US waves with higher frequencies (>2 MHz). In 1880, the brothers Pierre and Jacques Curie revealed their discovery about the piezoelectric phenomenon that was utilized afterwards to generate US waves with both low and high frequencies. They noticed that specific crystals like quartz, rochelle and tourmaline salt accumulate electric charge on their surface upon exposure to a mechanical pressure/tension [55]. In a reverse manner, a piezoelectric material vibrates when an electric charge is imposed on its surface. To further explore this phenomenon, let us consider a cylindrical bar of ceramic after polarization. When an electric field (i.e., voltage difference) is applied on the same direction of the poling voltage, the resulted

effect will be a total elongation of the bar. On the contrary, when the voltage direction is reversed, the bar will undergo a compression [56]. The other scenario is to translate a mechanical stress (tension/compression) into an electrical energy as shown in Figure 9-d, e. Generally, the main components required to construct a device that produces US waves are a transducer, a pulse generator and an amplifier. The transducer contains the piezoelectric material that translates electric pulses into mechanical vibrations. In medical scanning devices, a transducer also operates in the reverse direction receiving echoes (mechanical waves) and generating electric signals as a characteristic of the scanned medium. The pulse generator, as the name implies, generates regular electric pulses to be applied on the transducer, and allows the user to control the pulse frequency and amplitude, among other features. Finally, amplifiers are utilized in circuits basically to magnify the size of an electric signal. Other accessories may also be added to the circuit depending on the application.

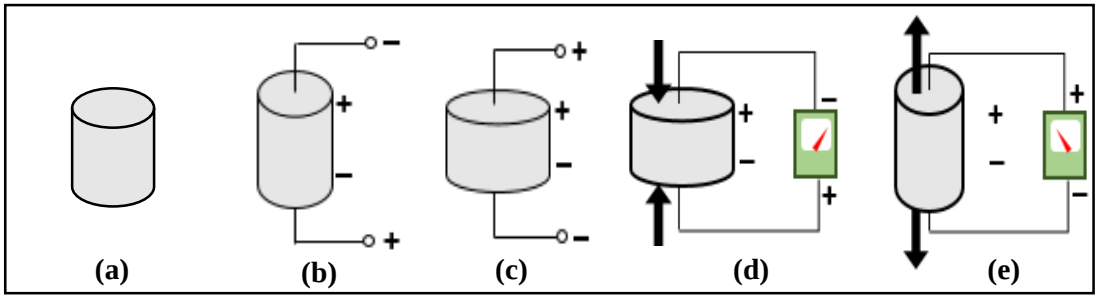

Figure 9: Piezoelectric effect. (a) Polarized segment, (b) stretched segment and (c) compressed segment due to voltage difference imposed, voltage produced due to (d) compression and (e) tension applied on the segment. Adapted from [56].

2.5.3. Physical properties of ultrasound.

The energy of US waves propagates through a medium by collisions of oscillatory particles but with no net displacement [57]. These waves can be focused, reflected and refracted. Ultrasound waves are sinusoidal waves with a given frequency, but when two waves of different frequencies interfere, their amplitudes are added/subtracted and the resulting frequency will be the result of the individual frequencies of each wave. Consequently, the superposition of waves can cause beats, and hence the wave is known to have a "beat frequency" that is coupled with Doppler effect in many applications. Doppler Effect is defined as the change of the wave frequency to a moving observer as he moves relative to the wave source. Once an US wave propagates into a medium, its amplitude diminishes, a phenomenon known as attenuation. Attenuation occurs due to several factors including the absorption of waves

resulting from the conversion of mechanical energy into heat, and the reflection and scattering of waves by irregular surfaces/interfaces. The intensity of the US beam is selected based on its application, as mentioned earlier. High-intensity US generates intense heat that is sufficient to melt steel [51]. In liquids, high-intensity US is associated with a phenomenon known as cavitation that is effectively used in drug delivery, as well as in cleaning processes.

Ultrasound waves are characterized by their frequency, propagation speed and amplitude. When an US wave propagates from one medium to another, both amplitude and velocity are affected, but the shape of the wave remains unchanged [58]. The velocity of a wave depends on the nature of the medium (its density and elasticity) and the type of the wave, while its amplitude depends on the impedance ratio of both mediums [51, 58]. Additionally, there are several modes of US vibration - longitudinal, transverse, torsion, shear, surface, flexural and Rayleigh - that can be utilized in ultrasonics applications [51]. Longitudinal waves (also known as compressional) are characterized by molecules vibration in parallel with the direction of energy transfer, while transverse waves are described by molecular vibrations that are orthogonal to the direction of energy transfer. Transverse waves can only propagate through a solid medium. On the contrary, gases can only transfer longitudinal waves, whereas liquids can transfer both longitudinal and surface waves. In biological-interaction systems, longitudinal waves are of special interest due to the favorable sequence of compressions and rarefactions created by these waves [59].

2.5.3.1. Acoustic impedance.

When an acoustic wave propagates through a fluid, the particles of that medium are forced to displace around their original position with a velocity known as *acoustic particle velocity* [60]. However, in any medium, there is a resistance to an acoustic wave propagation, which is called *acoustic impedance* (with SI units of $Pa.s/m^3$). Acoustic impedance is a key feature in determining the proportion of acoustic energy transmitted and reflected [61]. When the medium is characterized by closely-packed particles (i.e., dense material, high specific acoustic impedance), the particles require high pressure to move at a given velocity compared to a lower pressure requirement for loosely-packed materials (i.e., low specific acoustic impedance) at the same velocity (Eq.(1)) [62]. The equation that relates the pressure of an acoustic wave (P), the speed of sound in the

medium (c), the particle velocity (v) and the density of the medium (ρ) for which the wave is propagating through is [60]:

$$P = \rho . c . v = Z . v \quad \textbf{Eq. (1)}$$

Based on the equation above, the specific acoustic impedance (Z) (Pa.s/m equivalent to Rayl) for a substance is dependent on the density of the substance and the velocity of the acoustic wave. Table 2 lists the specific acoustic impedances for some materials and tissues [60].

Table 2: Characteristic acoustic impedance for selected biological tissues [60].

Tissue	Characteristic Acoustic Impedance (Rayls)
Water (20° C)	1.48×10^6
Muscle	$1.65 - 1.74\times10^6$
Fat	1.38×10^6
Skin	1.7×10^6
Cortical bone	$4 - 8\times10^6$

2.5.3.2. Reflection of waves.

When a wave strikes a boundary (e.g., a bone-tissue interface), the characteristic acoustic impedance of both media determines the fraction of the wave's energy to be reflected as an echo [61]. The difference between two medias' impedances is known as an *acoustic impedance mismatch* [62]. The greater the difference between the impedances, the more the acoustic energy is reflected from the interface, hence less energy is transmitted into the second medium. If the impedances of both media are identical, then there will be a complete transmission with no reflection. Besides the mismatch factor, the angle of the wave incidence also plays a role in determining the proportion of energy to be reflected and transmitted. When a beam is aimed on a surface at an orthogonal angle, the fraction of the reflected (R) and transmitted (T) energies for longitudinal waves is represented by the following [60],

$$R = (Z_1 - Z_2)^2/(Z_1 + Z_2)^2 \quad \textbf{Eq. (2)}$$

$$T = 4\, Z_1 Z_2/(Z_1 + Z_2)^2 \quad \textbf{Eq. (3)}$$

where Z_1 and Z_2 are the impedances of material 1 and 2, respectively. Based on Eqs. (2) and (3), it can be easily proved that the total sum of reflection and transmittance is equivalent to unity (R+T=1), hence the energy is conserved (lossless case). The reflection of waves is utilized in medical imaging to visualize tissues and organs. When

the acoustic mismatch is great, most of the waves are bounced back from the interface as a strong echo while the rest of the energy transmitted into the second medium cannot be used to produce images for inner organs and tissues. This is the reason why a transducer cannot acquire an image when there is a gap of air between the transducer and the patient's skin (case of total reflection of acoustic waves due to impedance discontinuity). Thus, a material with an intermediate acoustic impedance (gel or oil) must be placed between the transducer and the skin while imaging [60]. This justifies why air-filled organs block the tissues and organs underneath from imaging.

2.5.4. Ultrasound triggering.

Triggering in drug delivery is defined as the method that allows the control of drug release in its amount, location, and the period at which it is being released [63]. Several triggering techniques, such as pH, temperature, enzymes and light stimuli, have been suggested to release liposome-encapsulated drugs [64-67]. In addition to these techniques, research has shown that drug release can be controlled efficiently via US [68]. In liposomal drug delivery, US is utilized to control the release of a certain drug via mechanical and/or thermal effects. This technique of drug release is applied to echogenic and emulsion liposomes (eLiposomes). The two main parameters of US involved in triggering the release of drugs are the frequency and the intensity, as mentioned earlier. In drug delivery, the high-intensity focused US (HIFU) is used mainly in the release of drugs from temperature-sensitive liposomes, but HIFU can also treat (kill) tissues at elevated temperatures, a process known as hyperthermia [52]. Release of drugs can also be achieved using the non-thermal effects of low frequency US (LFUS). Kost *et al.* [69] demonstrated that the exposure to LFUS can increase the permeability of biological barriers (e.g., skin). This phenomenon has been used to increase the permeability of many biological barriers, such as cell membranes and tumors, thus facilitating the extravasation of drug into the desired site [70]. Schlicher *et al.* [71] showed that cell membranes can be disrupted via LFUS-induced cavitation. The LFUS results in transient pore-like disruptions in the membrane with diameters lower than 28 nm, and for a duration of several minutes, after which the cellular repair mechanism recovers the intact membrane configuration. In the area of drug delivery, HFUS waves are preferable since they can be easily focused as compared to LFUS waves, hence allowing to target infected tissues without affecting the surrounding ones [72].

Ultrasound is known to induce mechanical and/or thermal effects [72]. The mechanical effect is reflected in acoustic cavitation events. Acoustic cavitation refers to the formation and/or the activity of gas or bubbles in a medium being exposed to an oscillating pressure [73]. The bubbles are either originally present in the liquid, or may be newly formed when the pressure is lowered below the vapor pressure of the liquid [52, 63]. There are two types of acoustic cavitation: *stable* and *collapse*. Stable cavitation describes the continuous oscillation of bubbles being exposed to an oscillating pressure, which in turn varies the bubble radius about an equilibrium value [52, 73]. The oscillation of bubbles shears the fluid and/or surfaces nearby [74]. The highest amplitude of oscillation occurs when the natural resonant frequency of bubbles matches that of the applied US wave [73]. Collapse cavitation, also known as transient cavitation, involves bubble oscillations with increasing amplitudes that lead to continuous expansion until exceeding the bubble resonant radius, beyond which the bubble grows suddenly and collapses vigorously [75]. The bursting bubbles in collapse/transient cavitation generate a short-lived intense local heating, which may reach up to 5000 K and is accompanied by high pressures, which can be as high as 1000 atm [76]. Although these very high temperatures can be achieved at a certain point, heating/cooling rates are very fast on the order of 10^{10} K/s, thus characterizing the cavitation as an adiabatic event [77]. Shortly after the bubble bursts, a high-velocity (several hundred meters per second) micro jet of liquid is produced that pushes surfaces nearby with massive energy. The resonant size of a bubble is dependent on the type of gas enclosed by the bubble and the characteristics of the US wave [78]. To initiate collapse/transient cavitation, an US power density threshold, proportional to frequency and is a characteristic of the bubble size, must be achieved [52]. As frequency decreases, the power density threshold also decreases which explains why collapse/transient cavitation occurs quite more often at low frequencies rather than at high frequencies [79]. In general, LFUS with high power density induces collapse/transient cavitation [80]. The consequences of collapse/transient cavitation may be detrimental to tissues and adjacent cells due to the huge shear stress, the shockwave produced and the free radicals generated at elevated temperatures that may interfere with biochemical processes [80, 81]. On the other hand, stable cavitation has no negative biological attributes and can be applied to enhance the convection of oxygen and nutrients into normal cells [82]. In liposomal drug release, stable cavitation is not as effective as collapse/transient cavitation. In order to use

collapse/transient cavitation in drug release, drawbacks of using this method should be minimized by selecting the suitable parameters of US. The key is to produce a bubble activity that effectively ruptures the liposomal membrane without damaging the adjacent endothelial cells or causing thrombosis [80].

Scientists have developed mechanical index (MI) to determine the occurrence of collapse/transient cavitation [83]. MI relates the peak negative pressure (P_r) during the rarefaction cycle of the wave to the square root of the wave frequency (f_o) according to the following equation [84]:

$$MI = \frac{P_r}{\sqrt{f_0}} \qquad \textbf{Eq. (4)}$$

The use of liposomes in conjunction with US as a trigger have been studied recently. The following sections summarize some representative research in this area.

2.6. *In vitro* Studies

In vitro studies investigating drug release from liposomes triggered by US aim to examine many factors which are either related to US or to the chemical nature of liposome constituents. The main parameters of US, affecting drug release, include wave frequency and power intensity, while the factors related to liposome nature include the lipid ratio, amount of grafted PEG, surface charge, etc. In this section, some of the studies concerning US-mediated drug release from liposomes are discussed.

A study conducted by Levi [85] investigated the release of doxorubicin (Dox) from Doxil® with different US frequencies. Doxil® is a liposomal anti-cancer drug that contains Dox loaded into stealth liposomes with 100 nm in diameter, and is one of the currently FDA-approved drug delivery formulations [86]. In the mentioned study, it was observed that exposing Doxil® to 20-kHz (1.2 W/cm^2) LFUS resulted in 85% and 61% release in saline and human sourced plasma, respectively [85]. At a higher frequency of 1 MHz (2.5 W/cm^2), the release occurred at a slower rate in saline and barely any release (5%) was observed in human plasma, while at 3 MHz no release was measured. According to the authors, the lower level of drug release in plasma was justified by the presence of plasma proteins that absorbed part of the US energy, thus reducing the potential of cavitation in liposomal membranes.

Another study, conducted by Afadzi *et al.* [83], showed that the release of the model drug calcein ($C_{30}H_{26}N_2O_{13}$) from DEPC-based liposomes was higher at low

frequency (300 kHz) than that measured at a higher frequency (1 MHz). The US frequency also shows a dependence on the size and lamellarities of liposomes, as suggested by Pong *et al*. [87]. When the size of liposomes is very small compared to the wavelength of US, the pressure gradient will not be sensed by the vesicle; instead, a uniform pressure will be detected. Thus, whether applying high frequency US (1 MHz, λ=1.5 mm) that is 4 orders of magnitude greater than a 100 nm liposome, or applying a LFUS (20 kHz, λ=75 mm) that is 5 orders of magnitude greater than a 100 nm liposome, may have a similar effect on drug release. However, based on experimental data, it was observed that a better release was achieved when using LFUS, which may be explained by the fact that LFUS requires lower power density to initiate collapse/transient cavitation [52].

Other studies showed that the US-mediated drug release from sonosensitive liposomes also depends on the membrane structure of these vesicles [88]. Evjen *et al.* [88] found that DOPE-based liposomes with DSPE-PEG_{2000} and cholesterol achieved a higher Dox release upon exposure to LFUS (40 kHz) as compared to DSPE and PC-based liposomes in 20% serum.

Evjen *et al.* [89] studied the mechanism of drug release from liposomes induced by US using cryogenic transmission electron microscopy (Cryo-TEM). It was suggested that, if the morphology and size distribution of the vesicles remain the same, before and after US exposure, then sonoporation (pore-mediated release) has a major role in the process. On the contrary, if the vesicles disintegrate into a smaller size, then temperature effects play a predominant role. It was also observed that inclusion of PEG within the liposomal membrane structure increased the drug release since PEG molecules absorb more US than lipid molecules do, hence increasing the events of cavitation [52].

In this thesis, the release of calcein from estrone-anchored stealth liposomes under the effect of US was studied. According to Paliwal *et al.* [12], the non-triggered release of drug from this type of liposomes, achieved over a period of 24 h, determined by the dialysis tube method, was 53.6±1.23 % for the ES-SL-Dox as compared to 47.3±1.34 % release from SL-Dox.

2.7. *In vivo* Studies

Evjen *et al.* reported an *in vivo* study using a mice model implanted with a prostate tumor. They used phthalocyanine chloride tetrasulphonic acid ($AlPcS_4$)

encapsulated in PEGylated liposomes, exposed the tumor site to 1.1-MHz US, and monitored the release of the compound by an increase in fluorescence [90]. They observed an increase in fluorescence up to 100%, which implies an efficient release of the drug. Other *in vivo* studies considered the concept of hyperthermia when using HIFU. Ranjan *et al.* [91], for example, studied the effect of HIFU on the drug release from low temperature sensitive liposomes (LTSL). In this study, LTSL and free Dox were administered intravenously in rabbits implanted with VX2 carcinoma cells. The concentration of Dox was found to be higher in tumors exposed to LTSL (8.8±1.4 μg Dox/g tissues) than in tumors treated with free Dox (4.0±1.0 μg Dox/g tissues). In another study, Seynhaeve *et al.* [92] investigated the uptake of Doxil® by melanoma BLM tumor implanted in mice. Also in this case, the results showed that the uptake of Doxil® by the tumor was higher than that of free Dox. However, this did not guarantee the cytotoxicity of the drug, since it had to be released to be effective in killing malignant cells. Thus, the same group also performed cytotoxicity and bioavailability experiments for both Doxil® and free Dox using human and mice melanoma cells. Cells treated with free Dox for 8 h resulted in an accumulation of 26% of the initial amount in the nucleus, thus killing the cells effectively, while only 0.5% of the initial concentration was detected in the cell cytoplasm. In comparison, cells treated with Doxil® for 8 h achieved only 0.4% accumulation of the available drug in nucleus, revealing the low cytotoxicity of Doxil®, when administered without an external stimulus, which is necessary to release the entrapped drug.

A study conducted by Paliwal *et al.* [12] on female BALB/c mice showed a greater uptake for estrone-targeted stealth liposomes in breast and uterus *versus* that of stealth liposomes without a targeting moiety. The greater accumulation of the liposomal formulation was attributed to the receptor-mediated endocytosis in response to estrone presence. The group also performed a test to evaluate the antitumor activity on a MCF-7 xenografted in nude mice. They found that ES-SL-Dox formulation had the greatest effect in inhibiting the tumor growth.

2.8. Emulsion Liposomes (eLiposomes)

Ultrasound, as a triggering technique, works best when gas bubbles are present. This requires stabilized microbubbles to release drug upon exposure to US, which has a major limitation since stable bubbles cannot be formed at sizes below 1 μm [93]. Based

on this, bubbles of bigger sizes will not be able to leak through tumors endothelium (via the EPR effect as discussed earlier); instead, they will remain circulating in circulatory system till they get opsonized. Ultrasound, as an active targeting technique, provides a good control over the timing and the rate of drug release. When liposomes are exposed to US, microbubbles close to liposomes are the factor responsible for cavitation that shears and ruptures liposomes [93]. However, since gas bubbles cannot extravasate into tumor tissues, it is essential to synthesize liposomes with high sensitivity to US, without depending on the existence of adjacent gas bubbles. This can be achieved by synthesizing liposomes with vaporizable emulsion droplets termed as emulsion liposomes or eLiposomes. The emulsion in these liposomes is of nanosize and made of perfluorocarbons (e.g. perfluorohexane PFC_6, perfluoropentane PFC_5) with high vapor pressures at biological temperatures, making liposomes responsive to low US intensities. The normal boiling points for PFC_5 and PFC_6 are 29 ^{o}C and 56 ^{o}C, respectively [94]. Unlike gas bubbles, these emulsions can be formed at stable nanoscale sizes [93]. Husseini *et al.* [94] studied the stability of calcein-encapsulating eLiposomes with PFC_5 emulsion and showed that barely any calcein was released at body temperature (37 ^{o}C), even though it is above the boiling point of the mentioned emulsion. This was justified by the fact that the apparent boiling point of the emulsion is actually higher due to the additional pressure, known as Laplace pressure, imposed by the lipid sphere containing the emulsion. Thus, when eLiposomes were incubated at higher temperatures in the study, the release increased significantly. According to the authors, the formation of gas bubbles was the proposed mechanism of release. Thus, it is a plausible idea to combine eLiposomes with US to initiate drug release. When eLiposomes are exposed to US, and during the low pressure phase of the US wave, the local pressure drops below the high pressure of emulsions which is translated to a change in the phase of the emulsion to a vapor phase that expands and bursts the membrane of the liposome to release some of the drug encapsulated [93].

Chapter 3: Experimental Procedure

The first step in this work was the preparation of liposomes, according to a modified lipid film hydration method described by Torchilin and Weissig [33]. A method was developed to prepare the DSPE-PEG-estrone lipid derivative, and the targeting moiety was detected by Infrared Spectroscopy (IR). The size of the liposomes was determined by Dynamic Light Scattering (DLS). Finally, the US-triggered release of a model drug (calcein) from the prepared liposomes was studied at both low frequency (20 kHz) and high frequency modes (1.07 MHz and 3.24 MHz).

The liposomes used in this study were prepared from 1,2-distearoyl-*sn*-glycero-3-phosphoethanolamine-N-[amino(polyethylene glycol)-2000] (DSPE-PEG_{2000}-NH_2) modified with estrone, and cholesterol, in addition to 1,2-dipalmitoyl-*sn*-glycerol-3-phosphochloine (DPPC). Poly(ethylene) glycol has a crucial rule in prolonging the circulation time for nanocarrier encapsulated drugs, as mentioned earlier [35]. The effect of incorporating cholesterol in lipids depends on the type of lipids, as illustrated by Mirafzali [95]. For unsaturated lipids (i.e., with double bonds), the high fluidity of these lipids is suppressed by adding cholesterol, hence their water permeability decreases and their stability increases. On the other hand, saturated lipids (e.g. DSPE, DPPC), which are used in this work, behave differently when cholesterol is added since they are more gel-like which makes them leak-poof even in the absence of cholesterol. Basically, the addition of cholesterol to saturated lipids aims to reduce the phase transition temperature. In this work, two types of liposomes were synthesized: the control batch of liposomes (without the targeting moiety), and the targeted liposomes (with targeting moiety anchored to their surface). The synthesis of targeted liposomes started with the reaction of cyanuric chloride $(NCCl)_3$ with estrone (ES) to form the targeting moiety ES-$N_3C_3Cl_2$. Then, the previously formed conjugate was reacted with DSPE-PEG_{2000}-NH_2 to form DSPE-PEG_{2000}- N_3C_3Cl-ES that was later reacted with DPPC and cholesterol to form liposomes. The synthesis of control liposomes was carried out using a similar synthesis scheme but with DSPE-PEG_{2000}-NH_2 instead of DSPE-PEG_{2000}-N_3C_3Cl-ES.

3.1. Materials

The DPPC and DSPE-PEG_{2000}-NH_2 (ammonium salt) were obtained from Avanti Polar Lipids Inc. (Alabaster, AL, USA). Sephadex G-100, estrone (ES), calcein disodium salt, potassium bromide (KBr), and 2,4,6 trichloro-1,3,5 triazine (cyanuric chloride $(NCCl)_3$) were obtained from Sigma-Aldrich (St. Louis, MO, USA). Triethylamine (TEA) was obtained from Reidel-de Haën (Germany). Chloroform was obtained from Panreac Quimica S.A. (Spain). Cholesterol was obtained from AlfaAesar (Ward Hill, MA, USA).

3.2. Preparation of DSPE-PEG-NH_2 and DSPE-PEG-$N_3C_3Cl_2$-ES Liposomes

3.2.1. Synthesis and IR analysis of estrone-$N_3C_3Cl_2$ chloride conjugate.

Prior to the liposomes preparation, ES was reacted with $(NCCl)_3$ to form a targeting moiety that later would be conjugated to DSPE-PEG_{2000}-NH_2. Estrone was reacted with $(NCCl)_3$ in a 1:1 molar ratio, in the presence of two molar equivalents of triethylamine (TEA), a chloride acceptor [96]. To achieve the mono-substitution of chlorine, the reaction was performed at 0^o C [96] for three hours. First, 2.45 mg of $(NCCl)_3$ were dissolved in a small amount of dry chloroform, in a round bottom flask. Then, a solution of 3.6 mg of ES dissolved in a suitable amount of dry chloroform was prepared in a vial, which was placed in an ice bath, prior to the addition of 3.7 µl of TEA. The round bottom flask containing the $(NCCl)_3$ solution was placed in an ice bath with magnetic stirring, and the ES solution was added dropwise. The flask was covered and the mixture was continuously stirred for three hours and cooled in an ice bath, then it was left stirring overnight at room temperature. Afterwards, the chloroform was dried under argon and the ES-$N_3C_3Cl_2$ conjugate was stored at -20° C until use. The reaction is shown in Figure 10.

The ES-$N_3C_3Cl_2$ conjugate was analyzed by IR to confirm if the desired product of the reaction was obtained. The potassium bromide (KBr) disk method was used to carry out the analysis [97]. Testing by IR was followed because the absorbance/transmittance of the hydroxyl group in the estrone molecule can be detected with its corresponding wave number as a peak in the IR spectra. Therefore, if the reaction occurred, the peak of the hydroxyl group will disappear. Immediately before starting the test, the KBr powder was dried due to their hygroscopicity, which adversely affects the analysis. First, 150-200 mg of spectrophotometric-grade KBr powder was ground to fine

powder in an agate mortar using a pestle. Then, a small amount of ES-$N_3C_3Cl_2$ (~0.1-2% of the KBr powder) was added and mixed with the KBr powder in the agate mortar. Afterwards, the powder was added carefully into the collar of a stainless-steel die assembly. The powder was then pressed for 2 minutes by placing the die into a hydraulic press (International Crystal Laboratories, Garfield, USA). Afterwards, the pressure was relieved gradually (to avoid breaking the formed disk), and the die was disassembled to remove the transparent disk which was placed carefully in a disk holder to be tested using an IR instrument.

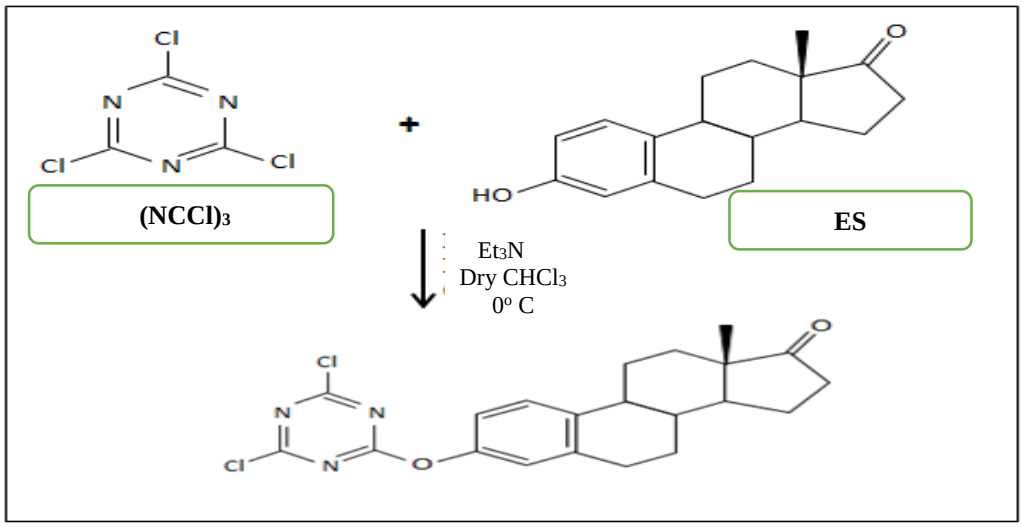

Figure 10: Synthesis of estrone-cyanuric derivative.

3.2.2. Synthesis of DSPE-PEG_{2000}-N_3C_3Cl-ES.

The previously prepared ES-$N_3C_3Cl_2$ derivative was reacted with DSPE-PEG_{2000}-NH_2 in a 1.2:1 molar ratio, in the presence of two molar equivalents of TEA, refer to Figure 11. To prepare DSPE-PEG_{2000}-N_3C_3Cl-ES for three batches of liposomes, 16.74 mg of DSPE-PEG_{2000}-NH_2 were dissolved in a small amount of dry chloroform, then 1.66 µl (12 µmol) of TEA were added dropwise and the vial was placed in an ice bath. The ES-$N_3C_3Cl_2$ conjugate was dissolved in 3 ml of dry chloroform and 1.72 ml (7.2 µmol) were transferred to a small round bottom flask placed in an ice bath. The DSPE-PEG_{2000}-NH_2 solution was then added dropwise and the mixture was kept stirring on ice for three hours, after which the stirring continued overnight at room temperature. If the prepared lipids were not used immediately, then chloroform was evaporated by purging with argon and stored at -20° C.

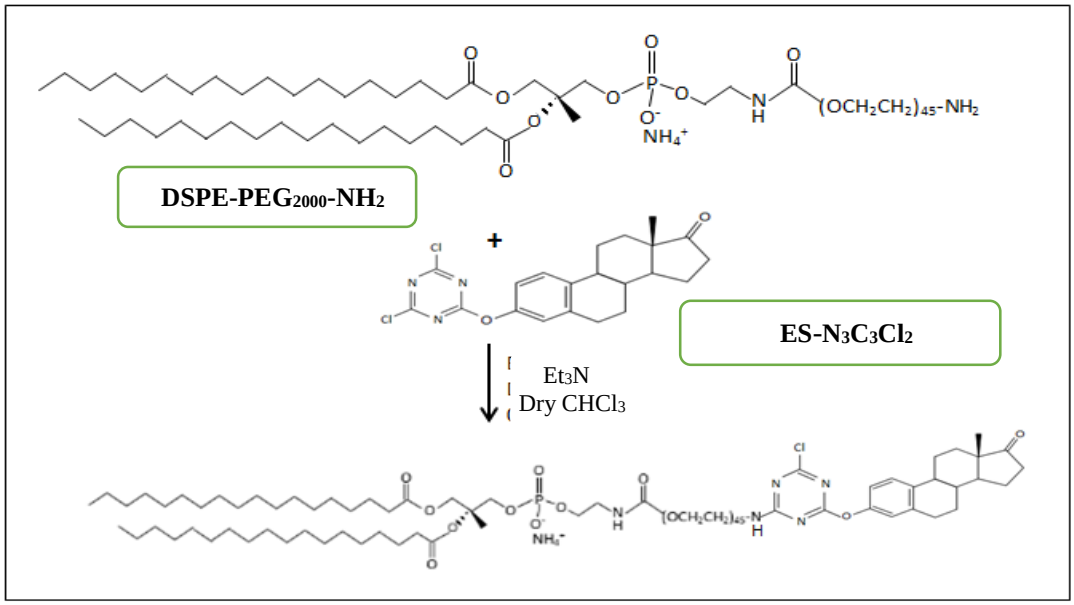

Figure 11: Synthesis of DSPE-PEG$_{2000}$-N$_3$C$_3$Cl-ES.

3.2.3. Preparation of DSPE-PEG$_{2000}$-N$_3$C$_3$Cl-ES liposomes encapsulating calcein.

Liposomes were synthesized at 60 ^{o}C (i.e., above the T_m of DSPE) using DPPC, cholesterol and DSPE-PEG$_{2000}$-N$_3$C$_3$Cl-ES at a molar ratio of 65:30:5, respectively. For one batch of liposomes, 2 µmol of DSPE-PEG$_{2000}$-N$_3$C$_3$Cl-ES were dissolved in 3 ml of dry chloroform in a round bottom flask, followed by the addition of 4.7 mg (12 µmol) of cholesterol and 19.2 mg (26 µmol) of DPPC. Chloroform was evaporated to dryness on a rotary evaporator at 60^{o} C for 15 minutes until a greasy-like film formed on the flask walls. The lipidic film was hydrated with 2 ml of 30 mM calcein in phosphate buffered saline (PBS) with the pH adjusted to 7.4. The solution was evaporated by rotating in a rotary evaporator without vacuum for 45 minutes, at 60^{o} C. Sonication was then performed in a 40-kHz sonicator bath (Elma D-78224, Melrose Park, IL, USA) at 60° C, for 15 minutes, after which the sample was extruded 30 times at the same temperature, using the Avanti® Mini-extruder with 0.2 µm polycarbonate filters (Avanti Polar Lipids, Inc., Alabaster, AL, USA). Liposomes were purified using a Sephadex G-100 gel filtration column (GE Healthcare Life Sciences), previously equilibrated with PBS, pH 7.4. The collected turbid liposome fractions were labeled and stored at 4° C until use.

3.2.4. Preparation of DSPE-PEG_{2000}-NH_2 (control) liposomes encapsulating calcein.

The steps followed to prepare control liposomes were similar to those described in Section 4.2.3 except that two molar equivalents of DSPE-PEG_{2000}-NH_2 were used instead of DSPE-PEG_{2000}-N_3C_3Cl-ES. The same molar ratio 65:30:5 DPPC:cholesterol:DSPE-PEG_{2000}-NH_2 was used.

3.3. Determination of Liposome Size by Dynamic Light Scattering (DLS)

The mean size of the liposomes was determined by Dynamic Light Scattering (DLS) using the DynaPro® NanoStar™ (Wyatt Technology Corp., Santa Barbara, CA, USA). The hydrodynamic radius (R_h) of the liposomes was determined at room temperature, after the liposome samples were properly diluted in PBS.

The principle of DLS is based on measuring the intensity of light scattered by the Brownian motion of molecules, as they diffuse, with respect to time. Besides the hydrodynamic radius, DLS measurements provide additional information related to size distribution and polydispersity of molecules in solution. Data obtained from Dynamic7 - Static, Dynamic, and Phase Analysis Light Scattering software were analyzed using two fits: cumulant and regularization [98].

Each fit has different implications and interpretation. A cumulant fit analyzes data with the assumption that particles exhibit unimodal distribution (i.e., they have similar average size). On the other hand, a regularization fit represents data with multimodal particle distribution. In this thesis, particles size determination of liposomes used a regularization fit, due the multimodality of the samples.

3.4. Low Frequency Ultrasound Release Studies (Online Experiments)

The release of calcein from liposomes was triggered using 20-kHz LFUS, and monitored by fluorescence changes using a QuantaMaster QM 30 Phosphorescence Spectrofluorometer (Photon Technology International, Edison NJ, USA). Calcein, a model drug, is a fluorescence molecule with excitation and emission wavelengths of 495 and 515 nm, respectively. As mentioned in Section 4.2.3, calcein was encapsulated as a 30 mM solution, which is a self-quenching concentration. Once US is applied, calcein is released from the liposomes to the surrounding medium, it gets diluted thus relieving the self-quenching, which can be monitored by an increase in fluorescence. The fluorescence of calcein is dependent on pH. Maherani *et al.* [99] found that the

fluorescence intensity (FI) of calcein decreases below pH 4.5, and that it is independent of pH between 6.5-10.

The liposomal suspension was diluted with PBS buffer (pH 7.4) in a fluorescence cuvette, which was then inserted in the spectrofluorometer chamber. The 20-kHz ultrasonic probe (model VC130PB, Sonics & Materials Inc., Newtown, CT) was inserted 2 mm into the cuvette through the specified opening of the spectrofluorometer. The initial fluorescence (F_i) was recorded for the first 60 s without sonication to generate a baseline. Then, sonication was turned on for a total of 13 min in a pulsed mode with 20 s *on* and 10 s *off*. Figure 12 clearly shows an increase in the fluorescence level during the *on* cycle (i.e., drug release occurs), while remaining in a plateau during the *off* cycle. In this thesis, three different machine power settings were examined at 20%, 25%, 30% which are equivalent to power densities of 6.08, 6.97, and 11.83 W/cm^2 [100, 101]. Finally, after approaching the maximum release (i.e., a plateau in release after 13 minutes), 2% (w/v) Triton X-100 (Tx100) was added to the sample cuvette (final concentration 0.48 mM) to lyse liposomes and release all the encapsulated calcein, which corresponds to fluorescence at 100% release. The percentage of calcein release was then calculated at a given time using the fluorescence intensity values obtained experimentally according to the following equation,

$$\%\ Drug\ Release = \frac{F - F_o}{F_{Tx100} - F_o} \times 100 \qquad \textbf{Eq. (5)}$$

where F is the fluorescence intensity at time (t) of insonation, F_o is the average of the initial fluorescence intensity before exposing the sample to US, and F_{Tx100} is the maximum fluorescence achieved after lysing liposomes with Tx100. For comparison analysis, data were further normalized.

3.5. High Frequency Ultrasound Release Studies (Offline Experiments)

High frequency release experiments were performed using 1.07-MHz and 3.24-MHz Ultrasonic probes (Precision Acoustics, Dorchester, UK) that are connected to an AC amplifier (High Voltage Amplifier WMA-300, Falco Systems, Amsterdam, The Netherlands). Samples were prepared similarly to those described in Section 4.4, i.e., the liposome suspension was diluted with PBS pH 7.4, in a fluorescence cuvette. The cuvette was placed in the fluorometer chamber to read the initial fluorescence intensity (baseline) for 1 min. Then, the liposome sample was transferred to a small beaker

partially immersed in a water bath at a certain distance above the suspended probe. The beaker was covered with parafilm to avoid any losses due to vaporization by US. The sample was sonicated under a continuous mode (in contrast to pulsed mode in LFUS release experiments), at a given frequency and voltage, for 10 minutes after which the sample was transferred to the fluorescence cuvette to record its fluorescence intensity for 1 min. The process was repeated every 10 min, for a total insonation time of 60 min. Afterwards, the detergent Tx100 was added to lyse the remaining liposomes and to record the maximum intensity of fluorescence, that corresponds to the final release.

In this work, the release was studied at 1.07 MHz at two power densities (10.5 and 50.2 W/cm^2), and at 3.24 MHz, at a power density of approximately 173 W/cm^2. The normalized percentage of drug release was calculated using Eq. (5), but the values of F_t and F_{Tx100} were substituted as averages over their period of insonation. Figure 13 shows, as an example, the fluorescence recorded for an experimental replicate followed by one sample calculation afterwards.

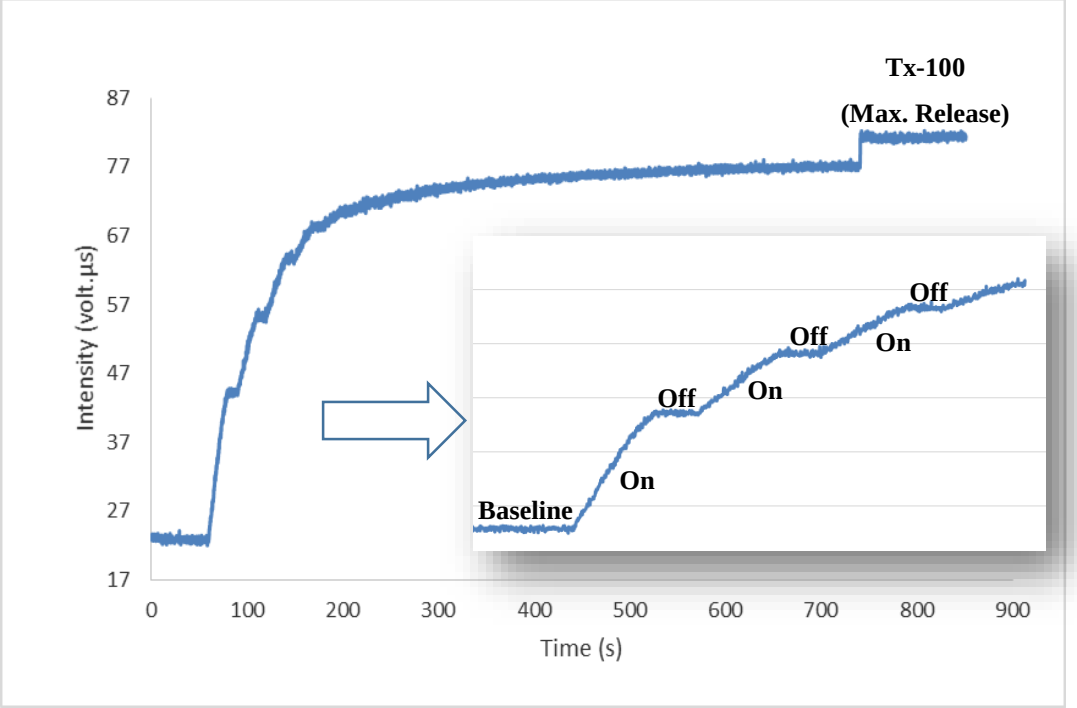

Figure 12: Online release experiment in a pulsed mode.

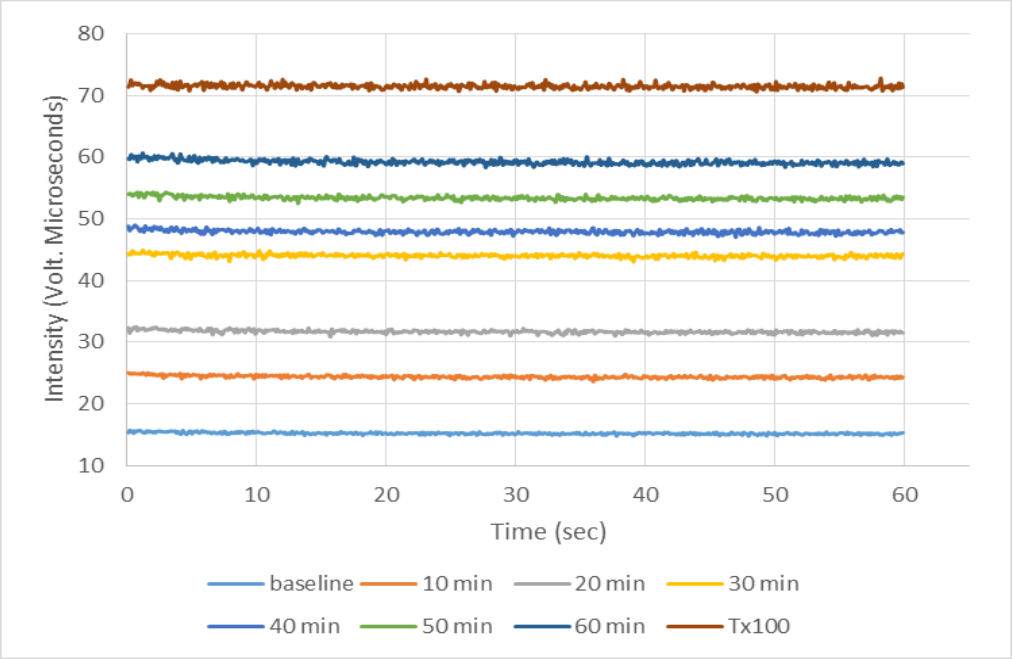

Figure 13: Fluorescence profiles for an offline experiment after 60 minutes of insonation with a 10-minute interval.

3.6. Statistical Analysis

The differences between results were compared using a two-tailed t-test with the assumption of unequal variances. Two values were considered significantly different when $p<0.05$ (unless otherwise stated).

Chapter 4: Results and Discussion

In this chapter, results will be presented and the corresponding discussion will be based on experiments conducted according to procedures outlined in chapter 4. Before preparation of liposomes, cyanuric chloride was attached to DSPE-PEG-NH_2 and estrone. Cyanuric chloride perform a di-substitution as reported by Blotny [96]. First, the targeting moiety, ES-$N_3C_3Cl_2$ was tested by an IR instrument, refer to Section 5.1. Then, particle size of both types of liposomes, control and ES-conjugated liposomes, was determined by DLS measurements, refer to Section 5.2. In the subsequent sections, low frequency and high frequency normalized release results were analyzed to study the effect of different power intensities and the role of the targeting moiety on drug release. Additionally, the type of cavitation incidents behind the release phenomenon was determined.

4.1. Infrared Spectra of the ES-$N_3C_3Cl_2$ Conjugate

Infrared spectra of estrone, cyanuric chloride and estrone-cyanuric conjugate were obtained to assess the reactivity of the hydroxyl group in estrone and to confirm whether the targeting moiety (estrone-cyanuric) was synthesized before reacting with DSPE-PEG_{2000}-NH_2. To test the outcome of the reaction, IR spectra of the reaction product (estrone-cyanuric) and reactants (estrone and cyanuric chloride) were obtained and are displayed in Figure 14. The alcohol group in estrone (at a stretching frequency of 3343.43 cm^{-1}) was not detected after the reaction which confirms the formation of the estrone-cyanuric conjugate.

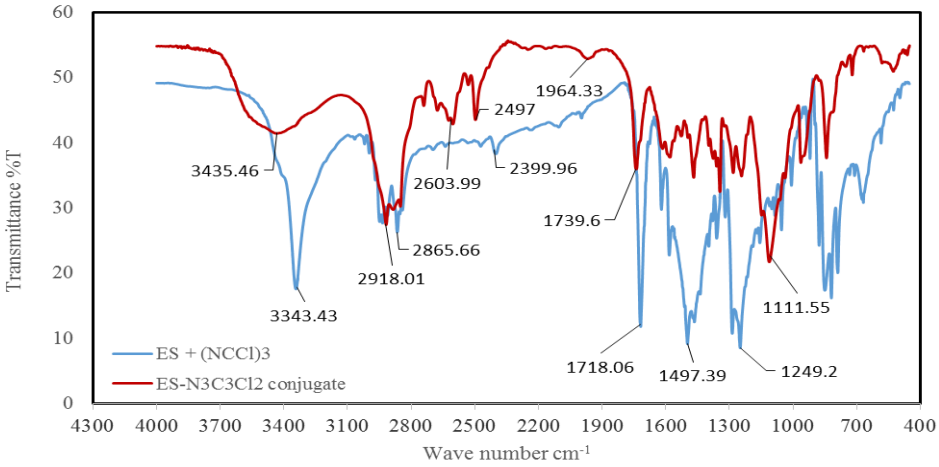

Figure 14: IR spectra of estrone and cyanuric chloride before the reaction (ES + $(NCCl)_3$) and the formed conjugate (ES-$N_3C_3Cl_2$) after the reaction.

4.2. Particle Size Measurements by DLS

The size of both control and ES-conjugated liposomes was determined by DLS according to the procedure outlined in Section 4.3. The results obtained are averages ± standard deviation of 3 different batches of liposomes. Based on the regularization fit, a radius of 92.9±15.8 nm was calculated for the ES-conjugated liposomes, while a radius of 96.75±3.83 nm was obtained for control liposomes. Thus, based on size, both types of liposomes are categorized as LUVs.

A two-tailed t-test with unequal variances was followed to test the significance of the type of liposomes on their size. It was found that there is no statistically significant difference between the sizes of both types of liposomes ($p>0.7$). The average polydispersity percentage (%Pd) for both types of liposomes was above 15% (24.0 ± 1.90% for ES-targeted liposomes, and 24.0 ± 1.43% for control liposomes), indicating a heterogeneous distribution of particles.

4.3. Low Frequency US-induced Release

4.3.1. DSPE-PEG_{2000}-NH_2 (control liposomes).

In release experiments, prior to starting the test, at least one sample (per batch) was utilized to generate the baseline and the maximum release (after adding Tx100) without any insonation. This provided an indication and validation of the maximum release for the following experiments.

In this section, two batches of control liposomes (3 replicates each) were insonated using a 20-kHz probe, and drug release was investigated at three power densities: 6.08, 6.97, and 11.83 W/cm^2 [100, 101]. The normalized averaged release profiles, highlighted with standard deviation, of control liposomes are shown in Figure 15. As can be seen, the initial rate of release increased with increasing power amplitudes during the first 200 seconds. After 13 minutes of pulsed insonation, Tx100 was added to lyse liposomes and fluorescence was measured for an additional 2 minutes to reach the maximum release. However, by adding Tx100, it was noticed that the fluorescence level was only slightly above the preceding plateau which indicates that liposomes have released most of their encapsulated calcein contents.

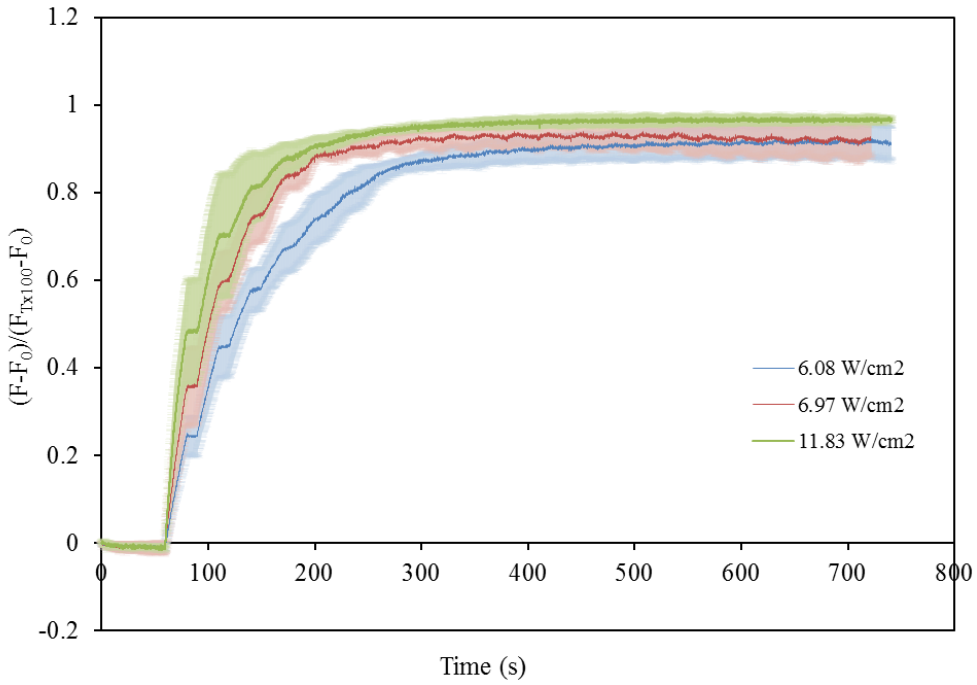

Figure 15: Normalized release profiles for DSPE-PEG$_{2000}$-NH$_2$ liposomes triggered by 20-kHz LFUS at the power densities indicated in the legend. Results are average ± standard deviation of 2 liposome batches (3 replicates each).

From the release curves shown in Figure 15, initial and final rates of release were calculated. The initial release rates were approximated by the normalized fluorescence values obtained after the first (60 to 90 sec) and second pulses (90 to 120 sec) of US. The final release was calculated after 13 minutes of pulsed insonation by adding Tx100 to lyse the remaining liposomes in solution. Figure 16 shows these results, which are also summarized in Table 3. The percentage of release after the first US pulse significantly increases ($p<0.05$) with power density: the percentage of release at 6.08 W/cm^2 is significantly lower ($p=5.87\times10^{-3}$) than the release obtained at 6.97 W/cm^2 and also significantly lower ($p=1.42\times10^{-6}$) than the one obtained at 11.83 W/cm^2. The release at 6.97 W/cm^2 is also significantly lower ($p=0.042$) than the one at 11.83 W/cm^2. Similar results were obtained when comparing the release after the second US pulse: the release significantly increases ($p<0.05$) with increasing power density. These results show that the release is faster for higher power densities.

The final percentages of release were very similar for all power densities, and the statistical analysis revealed that the differences between 6.08 and 6.97 W/cm^2 are not statistically significant ($p = 0.51$), however the release at 6.08 W/cm^2 is significantly lower ($p = 0.01$) than at 11.83 W/cm^2, and similarly, the release at 6.97 W/cm^2 is also significantly lower ($p = 0.04$) than at the highest power density employed in this work.

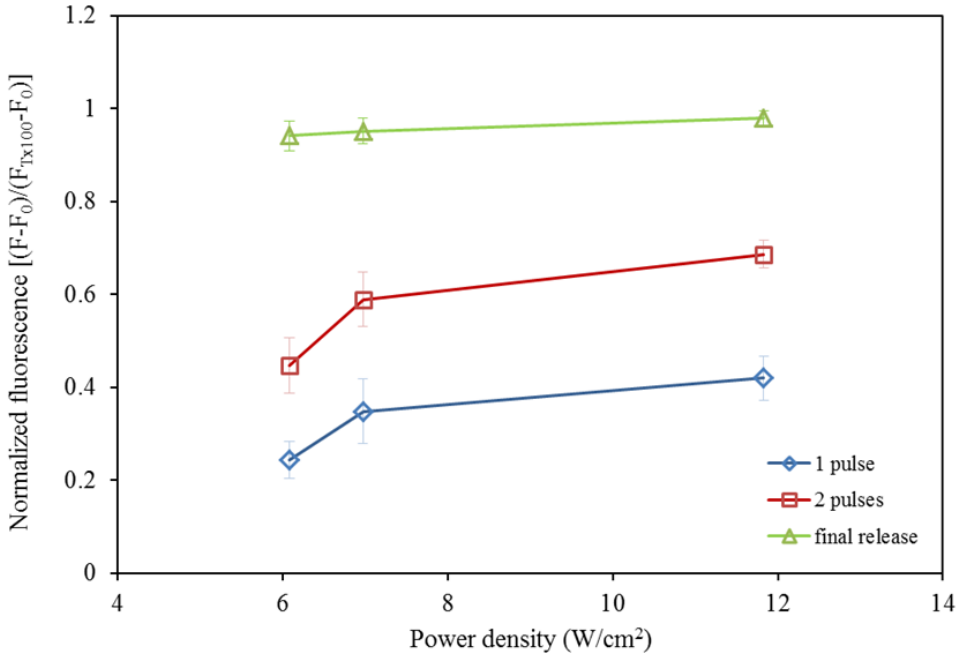

Figure 16: Normalized release profiles for DSPE-PEG$_{2000}$-NH$_2$ liposomes triggered by 20-kHz LFUS at 6.08, 6.97, and 11.83 W/cm^2. Results are average ± standard deviation of 2 liposome batches (3 replicates each), and are shown for first two pulses in addition to final release.

Table 3: Calcein release from DSPE-PEG$_{2000}$-NH$_2$ liposomes triggered by 20-kHz US at the indicated power densities. Results are average ± standard deviation of 2 liposome batches (3 replicates each).

Power density (W/cm^2)	Calcein release (% of normalized fluorescence)		
	Pulse #1	Pulse #2	Final Release
6.08	24.36 ± 3.88	44.77 ± 5.96	94.08 ± 3.19
6.97	34.84 ± 6.87	58.90 ± 5.89	95.13 ± 2.79
11.83	41.97 ± 4.72	68.61 ± 2.95	97.93 ± 1.53

Based on the mechanical index that was described in Section 2.5.4, collapse/transient cavitation is more likely to occur at low frequencies and high intensities, according to Eq. (4). Collapse/transient cavitation may also occur if the frequency is enough to counteract the effect of low power density. The MI threshold required to induce a collapse/transient cavitation is 0.7 as reported by Apfel and Holland [102] assuming the existence of free bubbles nearby. Using Eq. (4), the MI values calculated were 3.02, 3.23 and 4.21 for 6.08, 6.97 and 11.83 W/cm^2, respectively. Hence,

collapse/transient cavitation thresholds were achieved in all of the experiments. Referring to Figure 12, it is noticed that sonoporation of the liposomal membrane occurred during the phase of exposure to US. This is detected by an increase in fluorescence. On the other hand, the fluorescence ceased to increase once US is turned off indicating that the membrane restored its impermeability by healing its pores. Thus, it is expected that the release obtained at 20 kHz is mainly due collapse/transient cavitation as discussed by Schroeder *et al.* [103], Richardson *et al.* [104], and Lorenzo and Concheiro [105]. Schroeder *et al.* [52] reported that the power density threshold for cavitation induced by LFUS is approximately 1.2 W/cm^2 at 20 kHz. Evjen [106] further investigated whether liposomes disintegrate upon exposure to US by conducting an HPLC test on Dox-encapsulating DOPE-based and DSPE-based liposomes before and after exposure to 40-kHz and 1-MHz US. This analysis concluded that molecules of Dox, cholesterol and phospholipids did not disintegrate after being exposed to US but kept their chemical structure intact. Based on that, it is believed that sonoporation is the main mechanism for drug release from liposomes triggered by US, while the chemical integrity of lipids is preserved after exposure to US.

A comparison of the release from the DPPC-chol-DSPE-NH_2 liposomes studied here, with to DPPC-chol-DOPE-pNP liposomes previously synthesized in our group [100], showed that the release from the liposomes studied in this work occurs at a higher rate at each power density investigated, which may be either attributed to the type of lipids or due to the pNP group attached. In fact, the inclusion of DSPE in the liposome bilayer makes it more rigid [106], and hence more susceptible to rupture than DOPE because the former is a saturated lipid while the latter is an unsaturated lipid. The phase of a liposomal membrane is classified as a solid-ordered (SO) (also known as crystalline, or gel phase), liquid-disordered (LD) (also known as fluid, or liquid crystalline phase), or liquid-ordered (LO) [107]. The highest permeability is achieved when the membrane is in LD phase [52]. However, a membrane experiencing a phase transition is found to be more permeable than the LD phase because of having more than one phase at the same time, as reported by Jørgensen and Mouritsen [107]. Following this analysis, it is expected that a chaotic change in the membrane phase will result in a greater leakage (i.e., more drug release). Therefore, it is expected that higher release is obtained from saturated lipids than unsaturated ones since the former are more rigid and will result in a phase change from SO to LD once exposed to US. However, a study conducted by

Evjen claims that DOPE-based liposomes have a higher sonosensitivity to US than DSPE-based liposomes [106]. However, the author also showed that the incorporation of DSPE-PEG in DOPE-based liposomes enhances sonosensitivity, and has further concluded that the optimum membrane composition that would achieve the highest response to US should have DOPE, DSPE-PEG, and a low level of cholesterol [106].

4.3.2. DSPE-PEG_{2000}- N_3C_3Cl-ES liposomes.

For ES-targeted liposomes, an analysis similar to the one presented in Section 5.3.1 was performed, with results also obtained using two batches of liposomes (3 replicates each) sonicated at the same frequency and power densities. The release profiles are shown in Figure 17.

As seen in the case of control liposomes, the initial and final percentages of release were calculated from the obtained release curves (Figure 17), and the results are shown in Figure 18 and Table 4. In this case there are no significant differences ($p>0.05$) between the initial release rates (first and second US pulses) and the final release for the power densities 6.08 W/cm^2 and 6.97 W/cm^2. The releases after the first and second pulses are significantly higher for the highest power density, when compared to the 6.08 W/cm^2 ($p = 8.85x10^{-6}$ and $p=3.13x10^{-7}$, respectively) and to the ones obtained at 6.97 W/cm^2 ($p = 4.39x10^{-3}$ and $p=1.10x10^{-3}$, respectively). There were no statistically significant differences ($p>0.05$) of the final release percent for the three power densities studied. Furthermore, similarly to the discussion in Section 5.3.1, the mechanism of release is believed to be due to cavitation according to the calculated MI values tabulated in that section.

Table 4: Calcein release from DSPE-PEG_{2000}- N_3C_3Cl-ES liposomes triggered by the 20-kHz probe at the indicated densities. Results are average ± standard deviation of 2 liposome batches (3 replicates each).

Power density (W/cm^2)	Calcein release (% normalized fluorescence)		
	Pulse #1	Pulse #2	Final Release
6.08	39.42 ± 2.27	59.85 ± 3.30	97.13 ± 2.70
6.97	42.40 ± 8.74	65.34 ± 8.95	94.85 ± 5.47
11.83	54.96 ± 3.43	81.45 ± 2.65	98.69 ± 2.06

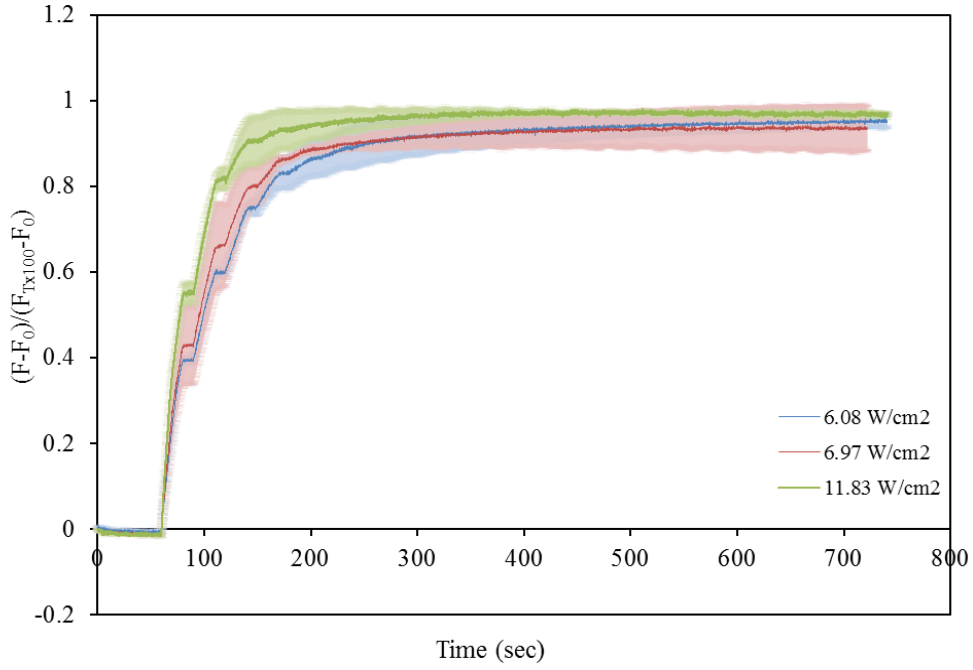

Figure 17: Normalized calcein release profiles from DSPE-PEG$_{2000}$- N$_3$C$_3$Cl-ES liposomes triggered by 20-kHz LFUS at the power densities indicated in the legend. Results are average ± standard deviation of 2 liposome batches (3 replicates each).

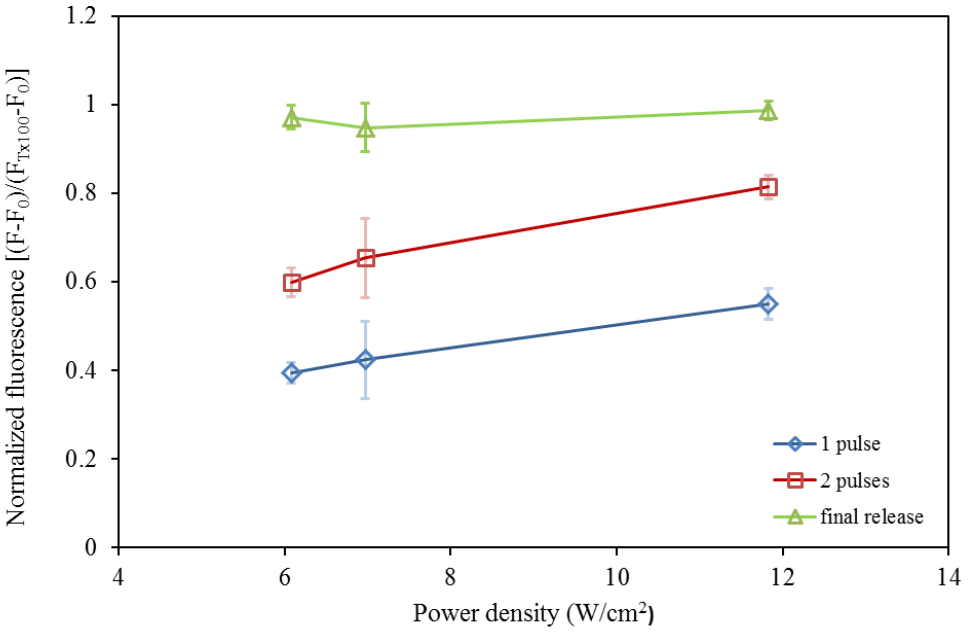

Figure 18: Normalized release profiles for DSPE-PEG$_{2000}$-NH$_2$ liposomes triggered by 20-kHz LFUS at 6.08, 6.97, and 11.83 W/cm^2. Results are average ± standard deviation of 2 liposome batches (3 replicates each), and are shown for first two pulses in addition to final release.

Researchers have conducted extensive studies in the area of micelles triggered with US [108-111] but studies using ES-conjugated liposomes are scarce. Paliwal *et al.* [12] investigated Dox release of a PC-based liposomal formulation with DPPE-PEG-ES using the dialysis tube method. Assuming that sonosensitivity is independent of the encapsulated chemical (i.e., Dox or calcein), as reported by Evjen [106], the maximum Dox release that was achieved by Paliwal for ES-conjugated liposomes using the dialysis tube method was 47.3 ± 1.34% after 24 h [106]. This release, and even higher, was easily achieved when the DSPE-PEG calcein-encapsulating liposomes, described in this work, were triggered with only one US pulse (20 s insonation), at a power density of 11.83 W/cm^2.

While no acoustically activated release from targeted liposomes have been previously reported in literature, US as a trigger has been used to stimulate release from targeted micelles. Initial release percentages for micelles were higher mainly because the structure of these drug delivery carriers is composed of a single layer (not a bi-layer as is the case with liposomes). In fact, 1-2 seconds were sufficient to cause approximately 8% release of doxorubicin from Pluronic® P105 micelles at 6 W/cm^2, and 70-kHz US [112]. The US release from micelles also showed a statistically significant difference between targeted and non-targeted micelles (with the targeted micelles showing higher release percentages) [112, 113]. There are three differences between acoustic micellar and liposomal release experiments. First, 70-kHz US was employed in the micellar experiments, while 20-kHz US was used for the liposomal experiments. Second, an actual chemotherapeutic drug was encapsulated inside the micelles as opposite to a model drug encapsulated inside liposomes. Third, the targeting moiety conjugated to the micelles was folic acid while in this study estrone was used to induce receptor mediated endocytosis via the use of targeted liposomes. Still a comparison is fruitful here, because both 20- and 70-kHz are in the low acoustic frequency range, Dox and calcein have similar molecular weights and aromatic rings, and both folic acid and estrone are low molecular weight targeting moieties. Finally, it should be noted that upon the termination of sonication, encapsulated drugs are re-encapsulated inside the micelles but not inside liposomes.

4.3.3. Comparison between ES-conjugated and control liposomes.

In this section, a comparison between control and ES-conjugated liposomes in terms of calcein release under the influence of US was investigated using the final release percent, as well as the release achieved after the first two pulses. Figure 19 shows a comparison between the averaged release profile of ES-conjugated and control liposomes at each power density. The comparisons between release after first pulse, second pulse and final release, for both types of liposomes, are shown in the histograms in Figure 20. A two-tailed t-test with unequal variances showed that there are no statistically significant differences ($p>0.05$) between the final releases from targeted and non-targeted liposomes at all power densities. On the contrary, targeted liposomes showed a significantly higher release than non-targeted liposomes at 6.08 W/cm^2 and 11.83 W/cm^2, after the first ($p=1.36\times10^{-6}$ and $p=6.63\times10^{-5}$, respectively) and the second US pulses ($p=6.64\times10^{-5}$ and $p=2.54\times10^{-6}$, respectively).

Estrone, which is very similar to cholesterol [114], is insoluble in aqueous solutions [115]. Hence, there is a great chance that some of the estrone molecules, that are anchored to the surface of liposomes, attempt to escape the surrounding medium (i.e., the aqueous PBS buffer) by incorporating themselves into the bilayer membrane. The inclusion of estrone molecules into a phospholipid membrane is believed to affect its nature as reported by Troxell *et al.* [114]. This may cause disorder and defects in the membrane of liposomes, which ultimately may facilitate release as sonoporation takes place.

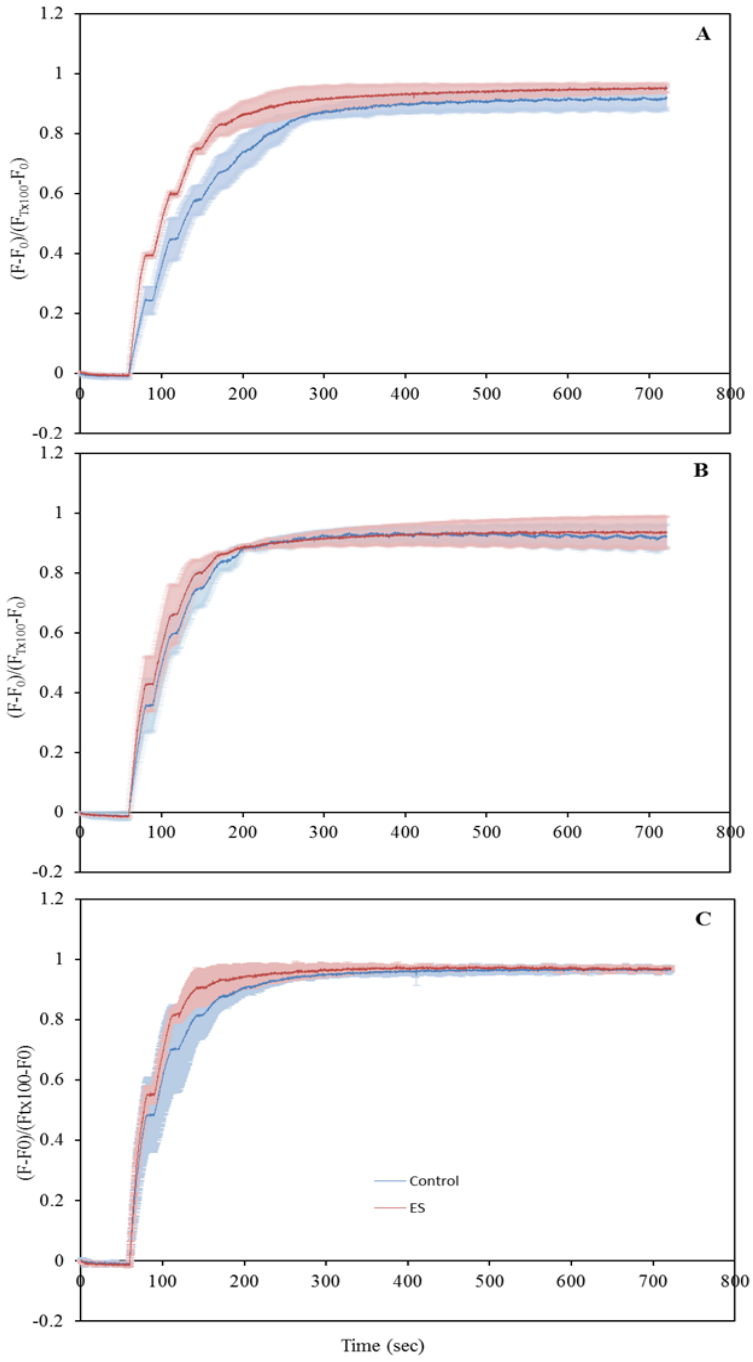

Figure 19: Comparison of the normalized calcein release profiles from DSPE-PEG$_{2000}$- N_3C_3Cl-ES and DSPE-PEG$_{2000}$-NH_2 liposomes triggered by 20-kHz LFUS at (A) 6.08 W/cm^2, (B) 6.97 W/cm^2 and (C) 11.83 W/cm^2. Results are average ± standard deviation of 2 liposome batches (3 replicates each).

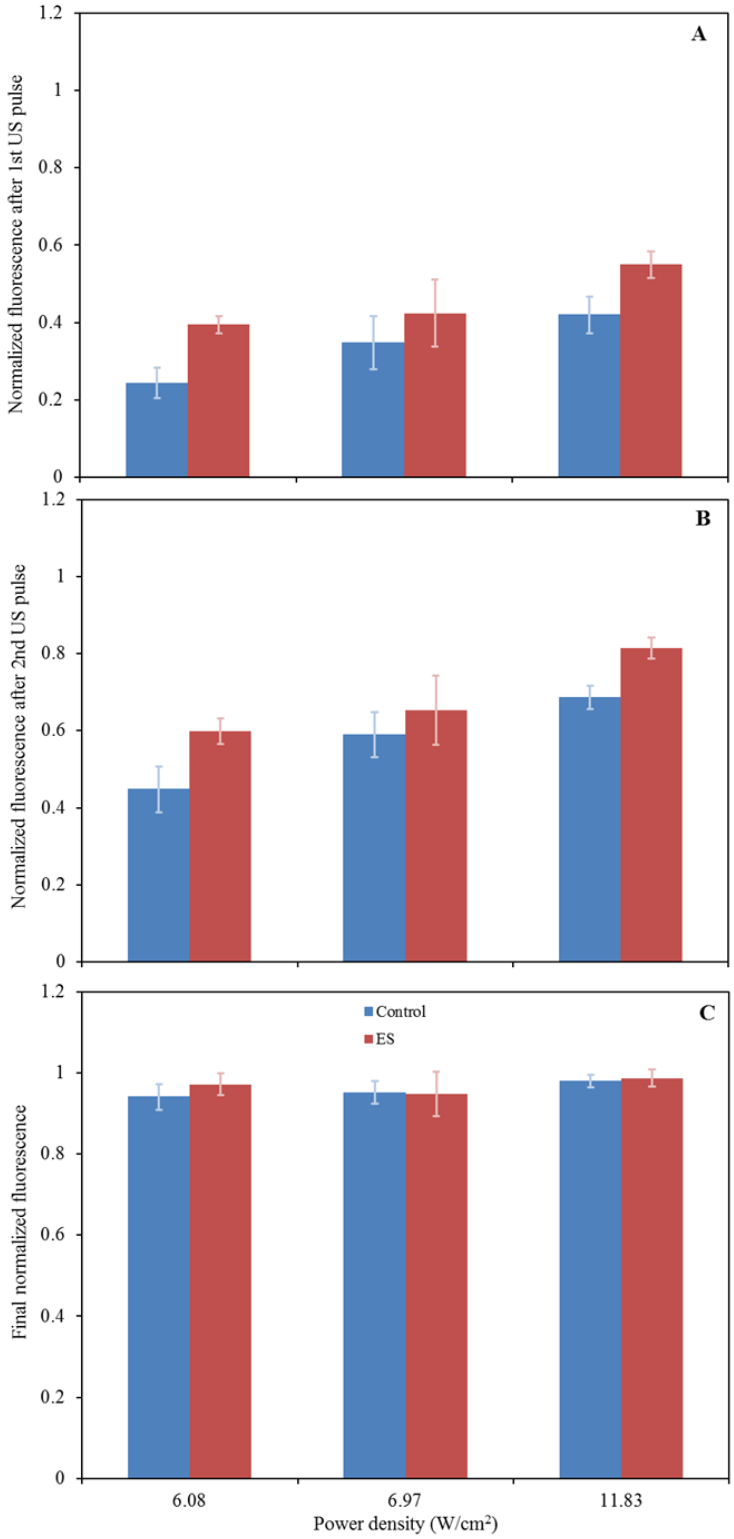

Figure 20: Comparison of calcein release from DSPE-PEG$_{2000}$-N$_3$C$_3$Cl-ES and DSPE-PEG$_{2000}$-NH$_2$ liposomes triggered by 20-kHz LFUS at the indicated power densities. (A) Release after the first US pulse, (B) release after the second US pulse, (C) final release.

4.4. High Frequency US Release

4.4.1. DSPE-PEG$_{2000}$-NH$_2$ (control liposomes).

In this section, the results of the HFUS-triggered calcein release from control liposomes, as described in Section 4.5, are described. High frequency US (HFUS) is a term used for US waves with frequencies higher than 1 MHz [52]. In this work, two high frequencies were tested, 1.07 MHz and 3.24 MHz, at two power densities (10.5 and 50.2 W/cm^2) for the former, and one power density (~173 W/cm^2) for the latter frequency. Two batches of control liposomes were sonicated at each power density, and at least three technical replicates were performed. The release profiles for both 1.07 and 3.24 MHz are shown in Figure 21.

When using 1.07-MHz HFUS, as shown in Figure 21, it was observed that the release significantly increased ($p<0.05$) with power density at each time point, except at 10 min. The release at 10.5 W/cm^2 was much lower than at 50.2 W/cm^2, and it barely showed an increase with time, ultimately reaching a final release of 8.45% after 60 min of insonation. On the other hand, the release at the higher power density (50.2 W/cm^2) showed a high rate of increase during the first 20 minutes of insonation, after which the increase continued at a slower rate. At this power density, the final release achieved after 60 min of insonation was 81.67%, approximately 10 times more than that achieved at 10.5 W/cm^2. At 1.07 MHz and 50.2 W/cm^2, it was noticed that the standard deviation is huge at the first 10 minutes of insonation. This is due to random attenuation of US waves as bubbles formed on the external surface of the beaker holding the sample.

The release profile at the higher frequency of 3.24 MHz showed a more sustained pattern of linear increase with time, but the calcein release after each 10-minute insonation is still less than that achieved when using the higher power density at 1.07 MHz, refer to Figure 21. Table 5 summarizes the average percentage of release for all power densities at the aforementioned frequencies.

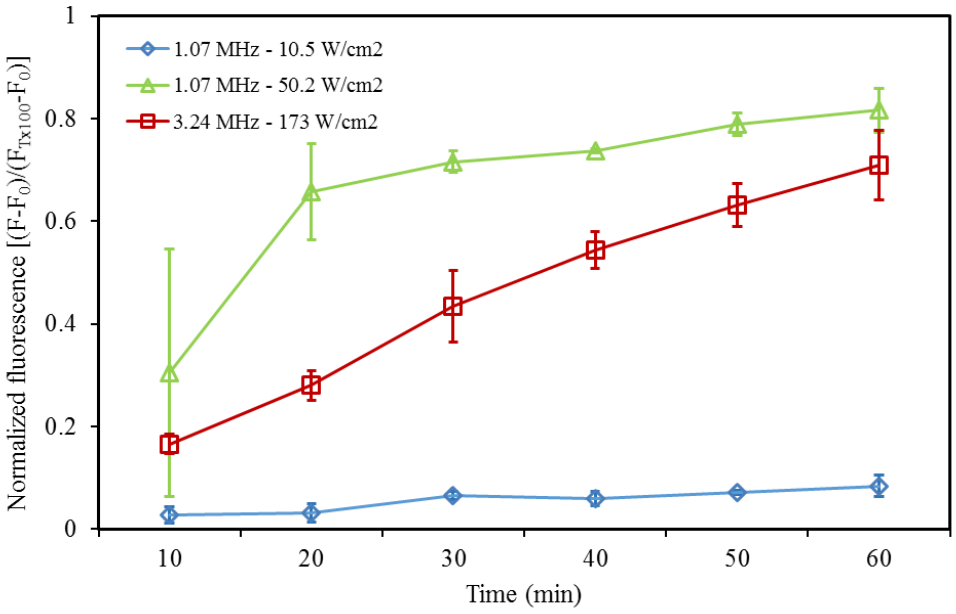

Figure 21: Normalized calcein release profiles from DSPE-PEG$_{2000}$- NH$_2$ liposomes, triggered by 1.07 and 3.24-MHz HFUS, at the two power densities indicated in the legend. Results are average ± standard deviation of 2 liposome batches (3 replicates).

Table 5: Calcein release from DSPE-PEG$_{2000}$-NH$_2$ liposomes triggered by the 1.07 and 3.24-MHz probes at 10.5, 50.2, and 173 W/cm^2 power densities. Results are average of 2 liposome batches (3 replicates each).

Time (min)	Calcein release (% normalized fluorescence)		
	1.07 MHz		3.24 MHz
	10.5 W/cm^2	50.2 W/cm^2	~173 W/cm^2
10	2.73	30.54	16.60
20	3.20	65.79	28.02
30	6.55	71.58	43.42
40	5.93	73.68	54.33
50	7.16	78.95	63.14
60	8.45	81.67	70.92

The mechanical indices were determined in a similar way to those calculated in the LFUS sections. The calculated MI values were 0.54, 1.19 and 1.27 for 10.5, 50.2 and 173 W/cm^2, respectively. At 10.5 W/cm^2, it was observed that only 8.45% calcein release was achieved after one hour of insonation which implies that collapse cavitation has not been achieved when compared to releases at the other two power densities. This is supported by the fact that the calculated MI at that power density is below the

threshold value for collapse cavitation (MI=0.54<0.7), hence release might have been induced by the effect of hyperthermia and/or stable cavitation. The mechanism of release at both 50.2 and 173 W/cm^2 is believed to be due to collapse/transient cavitation, since the corresponding MI values exceed the threshold value needed to induce cavitation. However, release was observed to be higher at 50.2 W/cm^2 as compared to release achieved at 173 W/cm^2 because higher frequency was used for the latter power density. The observation is consistent with the fact that attenuation of US waves increases as frequency increases [116]. Thus, to achieve a higher release at 3.24 MHz, power density should be increased to compensate for energy losses (i.e., heat dissipation). Based on literature, release is expected to be higher at LFUS than HFUS since cavitation events are easier to be induced at the former condition. The reason for this behavior is due to the fact that cavitation has more chance to occur when bubbles are given enough time to grow and collapse, which is achieved at LFUS because the time interval for the negative peak pressure is sufficient for nucleation [102].

The liposomes synthesized in this thesis are DPPC-based (i.e., the major lipid constituent), with a small fraction of DSPE-PEG and cholesterol. The transition temperature of DPPC is 41.5^o C [117], and the transition temperature of DSPE is even higher (74^o C) [118], but the inclusion of cholesterol counteracts the effect of DSPE by lowering the transition temperature of saturated lipids. Therefore, it is believed that hyperthermia may be one reason for permeating the membrane and for releasing calcein, especially at 3.24 MHz because the attenuation of US waves (and conversion to heat) increases with increasing frequency [105]. Another mechanism that may contribute to calcein release is "acoustic streaming," which has a mechanical effect rising from the partial absorption of US energy by the fluid. This energy is translated then to a convective flow in the direction of US propagation, thus inducing mixing and the collision of nanoparticles that may ultimately rupture the membrane and release encapsulated calcein.

4.4.2. DSPE-PEG$_{2000}$- N_3C_3Cl-ES (targeted liposomes).

Similar to the analysis conducted in Section 5.4.1, two batches (3 replicates each) of liposomes targeted with ES-$N_3C_3Cl_2$ conjugate were tested for release at the same two frequencies (1.07 and 3.24 MHz) and power densities. Insonation was conducted for 60 minutes in 10-min intervals, after which the fluorescence was recorded. The release

profiles at 1.07 MHz, shown in Figure 22, are similar to those obtained previously in Figure 21. Clearly, calcein release increases as the power density increased from 10.5 to 50.2 W/cm^2 at each time interval. As noticed in Figure 22, specifically at 50.2 W/cm^2, the calcein release increased at a higher rate during the first 30 minutes of insonation compared to that during the last 30 minutes. Similar behavior was also noticed with control liposomes. On the other hand, the release at 10.5 W/cm^2 showed a slight increase with time and reached a final release of only 21.51% compared to 79.31% at the higher power density. For all the time points, except the first 10 min, the release at 10.5 W/cm^2 was significantly lower ($p<0.05$) than at 50.2 W/cm^2.

The release at the higher frequency of 3.24 MHz (173 W/cm^2) exhibits a linear increase with time and the final release after one hour was 63.02%, which is lower than that achieved at 1.07 MHz, 50.2 W/cm^2. The mechanism of release is expected to be due to hyperthermia and/or stable cavitation at 10.5 W/cm^2 and collapse/transient cavitation at 50.2 and 173 W/cm^2, similar to the analysis proposed in Section 5.4.1. Additionally, acoustic streaming and hyperthermia may also have contributed to release at 3.24 MHz. Based on the t-test results shown, the release increases significantly with power density except for the first 10 minutes of insonation. Table 6 summarizes the average percentage of release for all power densities and frequencies.

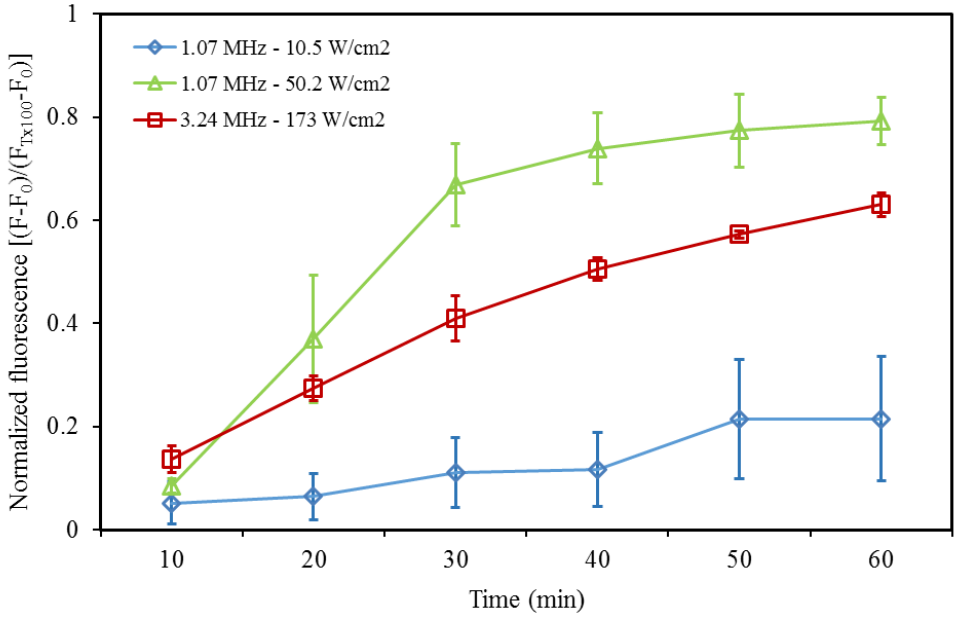

Figure 22: Normalized calcein release profiles from DSPE-PEG$_{2000}$-N$_3$C$_3$Cl-ES liposomes, triggered by 1.07 and 3.24-MHz HFUS, at the two power densities indicated in the legend. Results are average ± standard deviation of 2 liposome batches (3 replicates).

Table 6: Calcein release of DSPE-PEG$_{2000}$- N_3C_3Cl-ES liposomes triggered by the 1.07 and 3.24-MHz probes at 10.5, 50.2, and 173 W/cm^2 power densities. Results are average of 2 liposome batches (3 replicates each).

Time (min)	Calcein release (% normalized fluorescence)		
	1.07 MHz		3.24 MHz
	10.5 W/cm^2	50.2 W/cm^2	~173 W/cm^2
10	5.18	8.50	13.60
20	6.41	36.99	27.43
30	11.07	66.81	40.96
40	11.71	73.95	50.49
50	21.44	77.44	57.26
60	21.51	79.31	63.02

4.4.3. Comparison between ES-conjugated and control liposomes.

A comparison between ES-conjugated liposomes and control liposomes at each frequency and power density was also performed, and the results are presented in Table 7. No statistically significant differences were found between the two types of liposomes except at 1.07 MHz-10.5 W/cm^2, when the release from estrone liposomes was significantly higher ($p < 0.05$) at 50 and 60 min and after the 20 min of the 1.07 MHz-50.2 W/cm^2. Hence, the effect of the targeting moiety (ES-$C_3N_3Cl_2$) seems to be negligible, i.e., this targeting moiety does not interfere with release at HFUS. Figure 23 below shows all the release profiles for HFUS experiments.

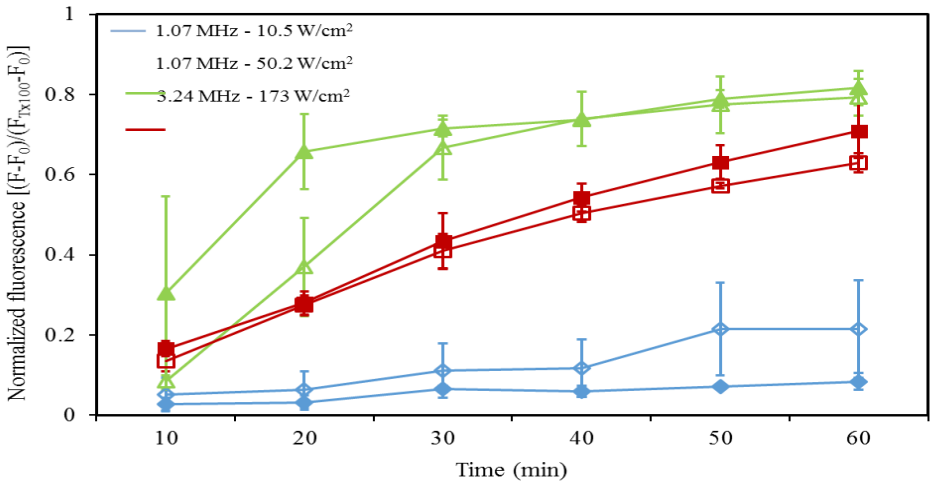

Figure 23: Comparison of the normalized calcein release profiles from DSPE-PEG$_{2000}$- N_3C_3Cl-ES and DSPE-PEG$_{2000}$-NH_2 liposomes triggered by 1.07 and 3.24-MHz HFUS, (◆) ES-1.07 MHz, 10.5 W/cm^2, (■) ES-1.07 MHz, 50.2 W/cm^2, (▲) ES-3.24 MHz, 173 W/cm^2, (◇) Control-1.07 MHz, 10.5 W/cm^2, (□) Control-1.07 MHz, 50.2 W/cm^2, (△) Control-3.24 MHz, 173 W/cm^2. Results are average ± standard deviation of 2 liposome batches

Table 7: T-test with unequal variances including the p-values to compare calcein release from ES-conjugated versus control liposomes triggered by the 1.07 and 3.24-MHz probes at 10.5, 50.2, and 173 W/cm^2 power densities

Time (min)	1.07 MHz		3.24 MHz
	10.5 W/cm^2	50.2 W/cm^2	173 W/cm^2
10	0.2465	0.2542	0.1903
20	0.1702	**0.0169**	0.8012
30	0.1661	0.3244	0.6374
40	0.1087	0.9424	0.2014
50	**0.0293**	0.7101	0.1329
60	**0.0452**	0.5198	0.1709

Chapter 5: Conclusion and Recommendations

Drug delivery systems are nanoparticles that are designed to transport cytotoxic drugs specifically to tumor sites to spare the surrounding tissues from the adverse effects associated with conventional chemotherapy. Liposomes are one of the nanocarriers that are being used to target tumors either by the EPR effect, or more selectively by attaching a targeting moiety that matches a receptor present on the surface of cancer cells. Once a nanocarrier reaches the target site, it requires a triggering stimulus to release its load. In this thesis, DPPC-based liposomes that encapsulate calcein and targeted with estrone-cyanuric conjugate were prepared as part of a potential treatment for breast cancer. Additionally, non-targeted liposomes were prepared and both types of liposomes were tested for calcein release in response to US triggering.

After preparing the liposomes according to the lipid film hydration method, the sizes of both, targeted and non-targeted, were determined by DLS and were found to be similar and categorized as LUVs. The LFUS release experiments showed no statistical significance in what concerns calcein final release, when comparing both types of liposomes at the same power amplitude/density. On the contrary, estrone-conjugated liposomes showed a significantly higher release during the first two US pulses at 6.08 and 11.83 W/cm^2 power densities in comparison to their non-targeted counterparts. By studying the effect of power densities on release, both types of liposomes reflected significantly higher release with increasing power densities during the first two pulses. However, final release showed a different response to power density for control liposomes compared to estrone-conjugated liposomes. Finally, regarding HFUS release experiments, all liposomes showed a significant increase in release with increasing power densities, but did not show a statistical significant difference when both types of liposomes were compared at a certain power density and frequency.

To extend this thesis further in the future, more *in vitro* release experiments are required with various power densities, especially at high frequencies which are more appealing for drug delivery researchers since waves can be easily focused at HFUS when compared to focusing at LFUS. Additionally, the investigation of doxorubicin release will further improve the utility of this drug delivery system. After collecting enough data, the dynamics of drug release can be modeled using mechanistic and stochastic models to provide us with a model that depicts and control the release at different

frequencies and power densities. Based on *in vitro* studies, the optimum parameters of US can be determined to be applied in cytotoxicity studies using human breast cancer cell line (MCF-7) and detected using a flow cytometer instrument. For *in vivo* studies, an important issue to be considered is the nature of estrone that is conjugated to the surface of liposomes. Estrone is a hydrophobic molecule, meaning that it will try to avoid the interaction with a surrounding medium if it is aqueous. In this work, estrone molecules are conjugated to PEG spacers that are attached to the surface of liposomes, thus these molecules will escape the aqueous medium by incorporating themselves in the membrane bilayer. This behavior will affect the ability of liposomes to target their receptors, and one proposed remedy would be to increase the spacer length (PEG) in order to hinder estrone from folding back to the lipid bilayer.

References

[1] "Cancer Statistics for 2014," American Cancer Soc., Atlanta, Georgia, Rep., 2014.

[2] D. L. Hoyert and J. Xu, "Deaths: Preliminary Data for 2011," National Vital Stat., Rep., 2012.

[3] "What Is Cancer? What Causes Cancer?" [Online]. Available: http://www.medicalnewstoday.com/info/cancer-oncology/, 2014 [Accessed: Sept. 15, 2014].

[4] D. Wujcik, "Science and mechanism of action of targeted therapies in cancer treatment.," *Semin. Oncol. Nurs.*, vol. 30, no. 3, pp. 139–146, Aug. 2014.

[5] "Timeline: Major Milestones Against Cancer | CancerProgress.Net," American Society of Clinical Oncology (ASCO), Alexandria, Virgina, Rep.

[6] T. A. Greenhalgh and R. P. Symonds, "Principles of chemotherapy and radiotherapy," *Obstet. Gynaecol. Reprod. Med.*, vol. 24, no. 9, pp. 259–265, Sep. 2014.

[7] M. Basel, "Targeting Cancer Therapy: Using Protease Cleavage Sequences to Develop More Selective and Effective Cancer Treatments." PhD Thesis, Kansas State University, USA, 2010.

[8] B. Colagiuri, H. Dhillon, P. N. Butow, J. Jansen, K. Cox, and J. Jacquet, "Does assessing patients' expectancies about chemotherapy side effects influence their occurrence?," *J. Pain Symptom Manage.*, vol. 46, no. 2, pp. 275–281, Aug. 2013.

[9] Z. Xu, H. M. Davis, and H. Zhou, "Rational development and utilization of antibody-based therapeutic proteins in pediatrics," *Pharmacol. Ther.*, vol. 137, no. 2, pp. 225–247, Mar. 2013.

[10] G. A. Husseini and W. G. Pitt, "Micelles and nanoparticles for ultrasonic drug and gene delivery," *Advanced Drug Delivery*, pp. 1137–1152, 2008.

[11] E. Cukierman and D. R. Khan, "The benefits and challenges associated with the use of drug delivery systems in cancer therapy.," *Biochem. Pharmacol.*, vol. 80, no. 5, pp. 762–770, Sep. 2010.

[12] S. R. Paliwal, R. Paliwal, N. Mishra, A. Mehta, and S. P. Vyas, "A Novel Cancer Targeting Approach Based on Estrone Anchored Stealth Liposome for Site-Specific Breast Cancer Therapy," *Current Cancer Drug Targets,* vol. 10, pp. 343-353, 2010.

[13] S. Rai, R. Paliwal, B. Vaidya, P. Gupta, S. Mahor, K. Khatri, A. Goyal, A. Rawat, and S.P. Vyas, "Estrogen(s) and Analogs as a Non-Immunogenic Endogenous Ligand in Targeted Drug/DNA Delivery," *Curr. Med. Chem.*, vol. 14, no. 19, pp. 2095–2109, Aug. 2007.

[14] A. Dickason and B. Waldera (2011, Mar. 9). *Polymeric Drug Delivery Systems - Biomaterials - UND Engineering* [Video file]. Available: http://www.youtube.com/watch?v=b5PhiT0C6h0, [Accessed: Sept. 19, 2014].

[15] S. Hauert and S. N. Bhatia,"Mechanisms of cooperation in cancer nanomedicine: towards systems nanotechnology," *Trends Biotechnol.*, vol. 32, no. 9, pp. 448–455, Jul. 2014.

[16] S. Venkataraman, J. L. Hedrick, Z. Y. Ong, C. Yang, P. L. R. Ee, P. T. Hammond, and Y. Y. Yang, "The effects of polymeric nanostructure shape on drug delivery," *Advanced Drug Delivery*, vol. 63, no. 14–15, pp. 1228–46, Nov. 2011.

[17] Y. Yeo, Ed. *Nanoparticulate Drug Delivery Systems: Strategies, Technologies, and Applications*. New Jersey: John Wiley & Sons, 2013.

[18] M. Fox, F. Szoka, and J. Frechet, "Soluble Polymer Carriers for the Treatment of Cancer : The Importance of Molecular Architecture," *Polymer Pharmacokinetics and Molecular Architecture*, vol. 42, no. 8, pp. 1141–1151, 2009.

[19] M. A. Elkhodiry, C. C. Momah, S. R. Suwaidi, D. Gadalla, A. M. Martins, R. F. Vitor, and G. A. Husseini, "Synergistic Nanomedicine: Passive, Active, and Ultrasound-Triggered Drug Delivery in Cancer Treatment," *Journal of Nanoscience and Nanotechnology*, vol. 15, pp. 1–19, 2015.

[20] P. J. Photos, L. Bacakova, B. Discher, F. S. Bates, and D. E. Discher, "Polymer vesicles in vivo: correlations with PEG molecular weight," *Journal of Controlled Release*, vol. 90, no. 3, pp. 323–334, Jul. 2003.

[21] H. Hatakeyama, H. Akita, K. Kogure, M. Oishi, Y. Nagasaki, Y. Kihira, M. Ueno, H. Kobayashi, H. Kikuchi, and H. Harashima, "Development of a novel systemic gene delivery system for cancer therapy with a tumor-specific cleavable PEG-lipid," *Gene Ther.*, vol. 14, no. 1, pp. 68–77, Jan. 2007.

[22] B. J. Staples, W. G. Pitt, B. L. Roeder, G. A. Husseini, D. Rajeev, and G. B. Schaalje, "Distribution of doxorubicin in rats undergoing ultrasonic drug delivery," *J. Pharm. Sci.*, vol. 99, no. 7, pp. 3122–31, Jul. 2010.

[23] D. Kim, A. D. Friedman, and R. Liu, "Tetraspecific ligand for tumor-targeted delivery of nanomaterials," *Biomaterials*, vol. 35, no. 23, pp. 6026–36, Jul. 2014.

[24] D. Lasic, "Liposomes synthetic lipid microspheres serve as multipurpose vehicles for the delivery of drugs, genetic material and cosmetics," *American Scientist*, vol. 80, no. 1, pp. 20–31, 1992.

[25] K. P. Kumar, D. Bhowmik, and L. Deb, "Recent Trends in Liposomes Used As Novel Drug Delivery System," *The Pharma Innovation International Journal*, vol. 1, pp. 26–34, 2012.

[26] G. P. Mishra, M. Bagui, V. Tamboli, and A. K. Mitra, "Recent applications of liposomes in ophthalmic drug delivery," *Journal of Drug Delivery*, vol. 2011, pp. 1-14, 2011.

[27] N. Monteiro, A. Martins, R. L. Reis, and N. M. Neves, "Liposomes in tissue engineering and regenerative medicine," *J. R. Soc. Interface*, vol. 11, no. 101, pp. 1–24, Oct. 2014.

[28] A. Porfire, I. Tomuta, L. Tefas, S. E. Leucuta, and M. Achim, "Simultaneous quantification of l-α-phosphatidylcholine and cholesterol in liposomes using near infrared spectrometry and chemometry," *J. Pharm. Biomed. Anal.*, vol. 63, pp. 87–94, Apr. 2012.

[29] A. Akbarzadeh, R. Rezaei-Sadabady, S. Davaran, S. W. Joo, N. Zarghami, Y. Hanifehpour, M. Samiei, M. Kouhi, and K. Nejati-Koshki, "Liposome: classification, preparation, and applications," *Nanoscale Res. Lett.*, vol. 8, no. 1, p. 102–110, Jan. 2013.

[30] P. R. Cullis, L. D. Mayer, M. B. Bally, T. D. Madden, and M. J. Hope, "Generating and loading of liposomal systems for drug-delivery applications," *Adv. Drug Deliv. Rev.*, vol. 3, no. 3, pp. 267–282, May 1989.

[31] J. Dua, A. Rana, and A. Bhandari, "Liposome: Methods of Preparation and Applications," *Int. J. Pharm. Stud. Res.*, vol. 3, no. 2, pp. 14-20, 2012.

[32] Y. P. Patil and S. Jadhav, "Novel methods for liposome preparation.," *Chem. Phys. Lipids*, vol. 177, pp. 8–18, Jan. 2014.

[33] V. Torchilin and V. Weissig. *Liposomes: A Practical Approach*. (2nd edition). Oxford: Oxford Univerisyt Press, 2003, pp. 3–12.

[34] F. Szoka and D. Papahadjopoulos, "Procedure for preparation of liposomes with large internal aqueous space and high capture by reverse-phase evaporation," *Proc. Natl. Acad. Sci. U. S. A.*, vol. 75, no. 9, pp. 4194–4198, Sep. 1978.

[35] M. L. Immordino, F. Dosio, and L. Cattel, "Stealth liposomes: review of the basic science, rationale, and clinical applications, existing and potential," *Int. J. Nanomedicine*, vol. 1, no. 3, pp. 297–315, Jan. 2006.

[36] J. W. Nichols and Y. H. Bae, "EPR: Evidence and fallacy," *J. Control. Release*, vol. 190, pp. 451–64, Sep. 2014.

[37] S. Stewart, K. Harrington, and M. Harrington, "The Biodistribution and Pharmacokinetics of Stealth Liposomes in Patients with Solid Tumors," *Oncology*, Oct. 1997.

[38] T. M. Allen, C. Hansen, F. Martin, C. Redemann, and A. Yau-Young, "Liposomes containing synthetic lipid derivatives of poly(ethylene glycol) show prolonged circulation half-lives in vivo," *Biochim. Biophys. Acta*, vol. 1066, no. 1, pp. 29–36, Jul. 1991.

[39] X. Wang, T. Ishida, and H. Kiwada, "Anti-PEG IgM elicited by injection of liposomes is involved in the enhanced blood clearance of a subsequent dose of PEGylated liposomes," *J. Control. Release*, vol. 119, no. 2, pp. 236–244, Jun. 2007.

[40] T. Ishida and H. Kiwada, "Accelerated blood clearance (ABC) phenomenon upon repeated injection of PEGylated liposomes," *Int. J. Pharm.*, vol. 354, no. 1–2, pp. 56–62, May 2008.

[41] X. Y. Wang, T. Ishida, M. Ichihara, and H. Kiwada, "Influence of the physicochemical properties of liposomes on the accelerated blood clearance phenomenon in rats," *J. Control. Release*, vol. 104, no. 1, pp. 91–102, May 2005.

[42] E. Forssen and M. Willis, "Ligand-targeted liposomes," *Adv. Drug Deliv. Rev.*, vol. 29, no. 3, pp. 249–271, Feb. 1998.

[43] V. Torchilin. *Multifunctional Pharmaceutical Nanocarriers*. New York: Springer Science & Business Media, 2008, p. 7.

[44] K. Maruyama, "Targetability of novel immunoliposomes modified with amphipathic poly(ethylene glycol) s conjugated at their distal terminals to monoclonal antibodies," *Biochim. Biophys. Acta - Biomembr.*, vol. 1234, no. 1, pp. 74–80, Mar. 1995.

[45] "Estrogens." [Online]. Available: http://www.webmd.com/women/estrogens, [Accessed: Dec. 5, 2014].

[46] M. Luconi, G. Forti, and E. Baldi, "Genomic and nongenomic effects of estrogens: molecular mechanisms of action and clinical implications for male reproduction," *J. Steroid Biochem. Mol. Biol.*, vol. 80, no. 4–5, pp. 369–381, Apr. 2002.

[47] L. Bjornstrom and M. Sjoberg, "Mechanisms of Estrogen Receptor Signaling: Convergence of Genomic and Nongenomic Actions on Target Genes," *Enocrine Soc.*, pp. 833–842, 2005.

[48] R. Lobo. *Treatment of the Postmenopausal Woman: Basic and Clinical Aspects*. (3rd edition). Academic Press, 2007, p. 767.

[49] D. L. Berkson. *Safe Hormones Smart Women*. Indiana: iUniverse, 2010, p. 31.

[50] S. Sarkar, S. Ali, L. Rehmann, G. Nakhla, and M. B. Ray, "Degradation of estrone in water and wastewater by various advanced oxidation processes," *J. Hazard. Mater.*, vol. 278, pp. 16–24, Aug. 2014.

[51] D. Ensminger and L. J. Bond. *Ultrasonics: Fundamentals, Technologies, and Applications.* (3rd edition). New York: CRC Press, 2011, pp. 1–52.

[52] A. Schroeder, J. Kost, and Y. Barenholz, "Ultrasound, liposomes, and drug delivery: principles for using ultrasound to control the release of drugs from liposomes," *Chem. Phys. Lipids*, vol. 162, no. 1–2, pp. 1–16, Nov. 2009.

[53] D. Ensminger. *Ultrasonics: Fundamentals, Technology, Applications, Second Edition, Revised and Expanded*. CRC Press, 1988.

[54] M. C. Jain. *Textbook Of Engineering Physics, Part 2*. New Delhi: PHI Learning Pvt. Ltd., 2010, pp. 239–241.

[55] S. N. Sen. *Acoustics, Waves and Oscillations*. New Delhi: New Age International, 1990, p. 204.

[56] I. Patel. (2011). "Ceramic Based Intelligent Piezoelectric Energy Harvesting Device," in *Advances in Ceramics-Electric and Magnetic Ceramics, Biocersmics and Environment*. [Online]. Available: http://cdn.intechopen.com/pdfs-wm/19252.pdf, [Accessed: Jan. 7, 2015].

[57] D. Martin, I. Wells, and C. Goodwin, "Physics of ultrasound," *Anaesth. Intensive Care Med.*, vol. 16, no. 3, pp. 132–135, Feb. 2015.

[58] B. M. Lempriere. *Ultrasound and Elastic Waves: Frequently Asked Questions*, vol. 13. San Diego: Academic Press, 2003.

[59] M. H. Repacholi, M. Gandolfo, and A. Rindi. *Ultrasound: Medical Applications, Biological Effects, and Hazard Potential*. New York: Plenum Press, 1987, p. 14.

[60] P. Laugier and G. Haiat. *Bone Quantitative Ultrasound*, vol. 30. New York: Springer Science & Business Media, 2010, pp. 32–39.

[61] P. Allisy-Roberts and J. R. Williams. *Farr's Physics for Medical Imaging*. Philadelphia: Elsevier Health Sciences, 2008, p. 153.

[62] V. Gibbs, D. Cole, and A. Sassano. *Ultrasound Physics and Technology: How, Why and When*. Elsevier Health Sciences, 2009, p. 21.

[63] H. G. Moussa, A. M. Martins, and G. A. Husseini, "Review on Triggered Liposomal Drug Delivery with a Focus on Ultrasound," *Curr. Cancer Drug Targets*, vol. 2, 2015.

[64] J. Connor, M. B. Yatvin, and L. Huang, "pH-sensitive liposomes: acid-induced liposome fusion," *Proc. Natl. Acad. Sci.*, vol. 81, no. 6, pp. 1715–1718, Mar. 1984.

[65] D. Needham, G. Anyarambhatla, G. Kong, and M. W. Dewhirst, "A New Temperature-sensitive Liposome for Use with Mild Hyperthermia: Characterization and Testing in a Human Tumor Xenograft Model 1," *Cancer Research*, pp. 1197–1201, 2000.

[66] J. E. Ghadiali and M. M. Stevens, "Enzyme-Responsive Nanoparticle Systems," *Adv. Mater.*, vol. 20, no. 22, pp. 4359–4363, Nov. 2008.

[67] O. Gerasimov, J. Boomer, M. Qualls, and D. Thompson, "Cytosolic drug delivery using pH- and light-sensitive liposomes," *Adv. Drug Deliv. Rev.*, vol. 38, no. 3, pp. 317–338, Aug. 1999.

[68] V. Frenkel, "Ultrasound mediated delivery of drugs and genes to solid tumors," *Adv. Drug Deliv. Rev.*, vol. 60, no. 10, pp. 1193–1208, Jun. 2008.

[69] J. Kost, K. Leong, and R. Langer, "Ultrasonically controlled polymeric drug delivery," *Die Makromol. Chemie. Macromol. Symp.*, vol. 285, pp. 275–285, 1988.

[70] A. Khaibullina, B.-S. Jang, H. Sun, N. Le, S. Yu, V. Frenkel, J. A. Carrasquillo, I. Pastan, K. C. P. Li, and C. H. Paik, "Pulsed high-intensity focused ultrasound enhances uptake of radiolabeled monoclonal antibody to human epidermoid tumor in nude mice," *J. Nucl. Med.*, vol. 49, no. 2, pp. 295–302, Mar. 2008.

[71] R. K. Schlicher, H. Radhakrishna, T. P. Tolentino, R. P. Apkarian, V. Zarnitsyn, and M. R. Prausnitz, "Mechanism of intracellular delivery by acoustic cavitation," *Ultrasound Med. Biol.*, vol. 32, no. 6, pp. 915–924, Jun. 2006.

[72] G. A. Husseini, W. G. Pitt, and A. M. Martins, "Ultrasonically triggered drug delivery: breaking the barrier," *Colloids Surf. B. Biointerfaces*, vol. 123, pp. 364–86, Nov. 2014.

[73] H. G. Flynn, "Physics of Acoustic Cavitation," *J. Acoust. Soc. Am.*, vol. 31, no. 11, p. 1582, Nov. 1964.

[74] M. Margulis. *Sonochemistry/Cavitation*. Amsterdam: Gordon and Breach Science, 1995, p. 311.

[75] T. Leighton, *The Acoustic Bubble*. Academic Press, 1994, p. 312.

[76] W. B. M. Iii, Y. T. Didenko, and K. S. Suslick, "Sonoluminescence temperatures during multi-bubble cavitation," *Nature*, vol. 401, pp. 772–775 October, 1999.

[77] A. E. Catania, A. Ferrari, M. Manno, and E. Spessa, “A Comprehensive Thermodynamic Approach to Acoustic Cavitation Simulation in High-Pressure Injection Systems by a Conservative Homogeneous Two-Phase Barotropic Flow Model,” *J. Eng. Gas Turbines Power*, vol. 128, no. 2, pp. 434–445, 2006.

[78] M. Keswani, S. Raghavan, and P. Deymier, “Characterization of transient cavitation in gas sparged solutions exposed to megasonic field using cyclic voltammetry,” *Microelectron. Eng.*, vol. 102, pp. 91–97, Feb. 2013.

[79] P. Hoskins, A. Thrush, K. Martin, and T. Whittingam. *Diagnostic Ultrasound: Physics and Equipment*. London: Cambridge University Press, 2003, p. 202.

[80] W. G. Pitt, G. A. Husseini, and B. J. Staples, “Ultrasonic drug delivery--a general review,” *Expert Opin. Drug Deliv.*, vol. 1, no. 1, pp. 37–56, Nov. 2004.

[81] L. Wang, J. H. Tay, S. Lee, and Y. T. Hung, Eds. *Environmental Bioengineering*. New York: Humana Press, 2010, p. 59.

[82] W. G. Pitt and S. A. Ross, “Ultrasound increases the rate of bacterial cell growth,” *Biotechnol. Prog.*, vol. 19, no. 3, pp. 1038–1044, 2003.

[83] M. Afadzi, C. D. Davies, Y. H. Hansen, T. Johansen, O. K. Standal, R. Hansen, S. E. Måsøy, E. A. Nilssen, and B. Angelsen, “Effect of ultrasound parameters on the release of liposomal calcein,” *Ultrasound Med. Biol.*, vol. 38, no. 3, pp. 476–486, Mar. 2012.

[84] J. Escoffre and A. Bouakaz. *Therapeutic Ultrasound*. Switzerland: Springer International, 2015, p. 278.

[85] C. Levi, “Ultrasound for targeted delivery of cytotoxic drugs from liposomes,” M.S. Thesis, Faculty of Engineering Science, Ben Gurion, Israel, 2000.

[86] G. Gregoriadis, Ed. *Liposome Technology: Entrapment of drugs and other materials into liposomes*. Boca Raton: Taylor & Francis Group, 2007, p. 2.

[87] M. Pong, S. Umchid, A. J. Guarino, P. A. Lewin, J. Litniewski, A. Nowicki, and S. P. Wrenn, “In vitro ultrasound-mediated leakage from phospholipid vesicles,” *Ultrasonics*, vol. 45, no. 1–4, pp. 133–145, Dec. 2006.

[88] T. J. Evjen, E. A. Nilssen, S. Barnert, R. Schubert, M. Brandl, and S. L. Fossheim, “Ultrasound-mediated destabilization and drug release from liposomes comprising dioleoylphosphatidylethanolamine,” *Eur. J. Pharm. Sci.*, vol. 42, no. 4, pp. 380–386, 2011.

[89] T. J. Evjen, S. Hupfeld, S. Barnert, S. Fossheim, R. Schubert, and M. Brandl, “Physicochemical characterization of liposomes after ultrasound exposure - mechanisms of drug release.,” *J. Pharm. Biomed. Anal.*, vol. 78–79, pp. 118–122, May 2013.

[90] T. J. Evjen, E. Hagtvet, A. Moussatov, S. Røgnvaldsson, J.-L. Mestas, R. A. Fowler, C. Lafon, and E. a Nilssen, “In vivo monitoring of liposomal release in tumours following ultrasound stimulation,” *Eur. J. Pharm. Biopharm.*, vol. 84, no. 3, pp. 526–531, Aug. 2013.

[91] A. Ranjan, G. C. Jacobs, D. L. Woods, A. H. Negussie, A. Partanen, P. S. Yarmolenko, C. E. Gacchina, K. V Sharma, V. Frenkel, B. J. Wood, and M. R. Dreher, "Image-guided drug delivery with magnetic resonance guided high intensity focused ultrasound and temperature sensitive liposomes in a rabbit Vx2 tumor model," *J. Control. Release*, vol. 158, no. 3, pp. 487–494, Mar. 2012.

[92] A. L. B. Seynhaeve, B. M. Dicheva, S. Hoving, G. A. Koning, and T. L. M. ten Hagen, "Intact Doxil is taken up intracellularly and released doxorubicin sequesters in the lysosome: evaluated by in vitro/in vivo live cell imaging," *J. Control. Release*, vol. 172, no. 1, pp. 330–340, Nov. 2013.

[93] J. R. Lattin, D. M. Belnap, and W. G. Pitt, "Formation of eLiposomes as a drug delivery vehicle," *Colloids Surf. B. Biointerfaces*, vol. 89, pp. 93–100, Jan. 2012.

[94] G. A. Husseini, W. G. Pitt, J. B. Williams, and M. Javadi, "Investigating the Release Mechanism of Calcein from eLiposomes at Higher Temperatures," *J. Colloid Sci. Biotechnol.*, vol. 3, no. 3, pp. 239–244, Sep. 2014.

[95] Z. Mirafzali, "Is it necessary to add cholesterol to a liposome formulation? - Quora." [Online]. Available: https://www.quora.com/Is-it-necessary-to-add-cholesterol-to-a-liposome-formulation, 2011 [Accessed: Oct. 5, 2015].

[96] G. Blotny, "Recent applications of 2,4,6-trichloro-1,3,5-triazine and its derivatives in organic synthesis," *Tetrahedron*, vol. 62, no. 41, pp. 9507–9522, Oct. 2006.

[97] M. Derrick, D. Stulik, and J. Landry. *Infrared spectroscopy in conservation science*, vol. 53. Los Angeles: J. Paul Getty Trust, 1999, p. 28.

[98] "How DLS works." [Online]. Available: http://wyatt.eu/index.php?id=how-dls-works, [Accessed: Oct. 9, 2015].

[99] B. Maherani, E. Arab-Tehrany, A. Kheirolomoom, D. Geny, and M. Linder, "Calcein release behavior from liposomal bilayer; influence of physicochemical/mechanical/structural properties of lipids," *Biochimie*, vol. 95, no. 11, pp. 2018–2033, Nov. 2013.

[100] S. Ahmed, "Dynamics of Chemotherapeutic Drug Release from Liposomes Using Low-Frequency Ultrasound," M.S. Thesis, Chemical Eng. Dept., American University of Sharjah, UAE, 2015.

[101] H. Moussa, "Liposomal Drug Release Using Ultrasound and Modeling Release Dynamics for Model Predictive Controller Design," M.S. Thesis, Electrical Eng. Dept., American University of Sharjah, UAE, 2015.

[102] R. E. Apfel and C. K. Holland, "Gauging the likelihood of cavitation from short-pulse, low-duty cycle diagnostic ultrasound," *Ultrasound Med. Biol.*, vol. 17, no. 2, pp. 179–185, Jan. 1991.

[103] A. Schroeder, Y. Avnir, S. Weisman, Y. Najajreh, A. Gabizon, Y. Talmon, J. Kost, and Y. Barenholz, "Controlling Liposomal Drug Release with Low Frequency Ultrasound : Mechanism and Feasibility," no. 19, pp. 4019–4025, 2007.

[104] E. S. Richardson, W. G. Pitt, and D. J. Woodbury, "The role of cavitation in liposome formation," *Biophys. J.*, vol. 93, no. 12, pp. 4100–4107, Dec. 2007.

[105] C. Lorenzo and A. Concheiro. *Smart Materials for Drug Delivery,* vol. 2. Cambridge: Royal Society of Chemistry, 2013.

[106] T. Evjen, "Sonosensitive liposomes for ultrasound-mediated drug delivery," PhD Thesis, Department of Pharmacy, University of Tromso, Norway, 2011.

[107] K. Jørgensen and O. G. Mouritsen, "Phase separation dynamics and lateral organization of two-component lipid membranes.," *Biophys. J.*, vol. 69, no. 3, pp. 942–954, Sep. 1995.

[108] G. A. Husseini and W. G. Pitt, "The use of ultrasound and micelles in cancer treatment," *J. Nanosci. Nanotechnol.*, vol. 8, no. 5, pp. 2205–2215, May 2008.

[109] J. Chandrapala, G. J. O. Martin, B. Zisu, S. E. Kentish, and M. Ashokkumar, "The effect of ultrasound on casein micelle integrity," *J. Dairy Sci.*, vol. 95, no. 12, pp. 6882–6890, Dec. 2012.

[110] A. Marin, H. Sun, G. A. Husseini, W. G. Pitt, D. A. Christensen, and N. Y. Rapoport, "Drug delivery in pluronic micelles: effect of high-frequency ultrasound on drug release from micelles and intracellular uptake," *J. Control. Release*, vol. 84, no. 1–2, pp. 39–47, Nov. 2002.

[111] N. Rapoport, "Ultrasound-mediated micellar drug delivery," *Int. J. Hyperth.*, vol 28, no. 4, pp. 374–385, May 2012.

[112] G. A. Husseini, L. Kherbeck, W. G. Pitt, J. a. Hubbell, D. a. Christensen, and D. Velluto, "Kinetics of Ultrasonic Drug Delivery from Targeted Micelles," *J. Nanosci. Nanotechnol.*, vol. 15, no. 3, pp. 2099–2104, Mar. 2015.

[113] G. A. Husseini, D. Velluto, L. Kherbeck, W. G. Pitt, J. A. Hubbell, and D. A. Christensen, "Investigating the acoustic release of doxorubicin from targeted micelles," *Colloids Surfaces B Biointerfaces*, vol. 101, pp. 153–155, 2013.

[114] E. Troxell, M. Troxell, and J. Bell, "The Effect of Estrone on the Interaction between Phospholipase A and the Phospholipid Bilayer," *J. Undergrad. Res. Brigham Young Univ.*, 2013.

[115] T. Boyer, D. Zakim, and D. Vessey, "Direct, Rapid Transfer of Estrone from Liposomes to Microsomes," *J. Biol. Chem.*, vol. 255, pp. 627–631, 1980.

[116] H. Azhari, *Basics of Biomedical Ultrasound for Engineers*. New Jersey: John Wiley & Sons, 2010, p. 96.

[117] A. Blume, "A comparative study of the phase transitions of phospholipid bilayers and monolayers," *Biochim. Biophys. Acta*, vol. 557, no. 1, pp. 32–44, Oct. 1979.

[118] G. Cevc and D. Marsh, "Phospholipid bilayers physical principles and models.," *Cell Biochem. Funct.*, vol. 6, no. 2, pp. 147–148, Apr. 1988.

Vita

Najla Mohammad was born on May 12, 1990, in Dubai, United Arab Emirates. She completed her primary, elementary, and high school in Sharjah. In 2008, Najla graduated from Al Heera Public School with 98.1%, and in 2009 she joined the American University of Sharjah to pursue a Bachelor Degree in Chemical Engineering and a Minor Degree in Petroleum Engineering. In 2013, she graduated with a Bachelor of Science in Chemical Engineering with Magna Cum Laude.

Immediately after Ms. Najla earned her bachelor degree, in 2013, she pursued a Master's Degree in Chemical Engineering at the American University of Sharjah. She was awarded a graduate assistantship that allowed her to work as a graduate teaching assistant from September 2013 until May 2015. After that, she worked as a research assistant from June until November 2015.

Ms. Najla is the coauthor of a paper entitled "*Effectiveness Design Parameter for Sedimentation of Calcium Carbonate Slurry*," that was published in the International Journal of Chemical, Environmental & Biological Sciences (IJCEBS) in 2013. And for the same paper, she was awarded the best speaker in a conference held in Dubai, 2013. In 2012, Ms. Najla attended the Abu Dhabi International Petroleum Exhibition and Conference (ADIPEC), Abu Dhabi, UAE, where she participated in various activities.